JB Journals.ASM.org

Defects in the Flagellar Motor Increase Synthesis of Poly-γ-Glutamate in *Bacillus subtilis*

Jia Mun Chan, Sarah B. Guttenplan, Daniel B. Kearns

Indiana University, Department of Biology, Bloomington, Indiana, USA

***Bacillus subtilis* swims in liquid media and swarms over solid surfaces, and it encodes two sets of flagellar stator homologs. Here, we show that *B. subtilis* requires only the MotA/MotB stator during swarming motility and that the residues required for stator force generation are highly conserved from the *Proteobacteria* to the *Firmicutes*. We further find that mutants that abolish stator function also result in an overproduction of the extracellular polymer poly-γ-glutamate (PGA) to confer a mucoid colony phenotype. PGA overproduction appeared to be the result of an increase in the expression of the *pgs* operon that encodes genes for PGA synthesis. Transposon mutagenesis was conducted to identify insertions that abolished colony mucoidy and disruptions in known transcriptional regulators of PGA synthesis (Com and Deg two-component systems) as well as mutants defective in transcription-coupled DNA repair (Mfd)-reduced expression of the *pgs* operon. A final class of insertions disrupted proteins involved in the assembly of the flagellar filament (FliD, FliT, and FlgL), and these mutants did not reduce expression of the *pgs* operon, suggesting a second mechanism of PGA control.**

Many bacteria swim in liquid or swarm over solid surfaces by rotating flagella. Flagella are complex molecular machines comprised of over 30 proteins that self-assemble to transit the cell envelope. Flagellar assembly begins with the basal body that serves as the membrane-anchored foundation and the secretion conduit for the subunits of the subsequent stages: the universal joint hook and the long helical filament (1). Once assembled, the filament is rotated like a propeller through a 360° angle at speeds of 100 to 1,000 revolutions per second (2). Flagellar rotation occurs when the energy of the proton motive force is converted into a physical interaction between the rotor, a ring of proteins connected to the flagellar basal body, and a series of 8 to 11 stator complexes anchored to the cell wall around the flagellum (3, 4, 5, 6, 7).

Each stator complex is composed of two proteins of MotB and four proteins of MotA (3, 8, 9). MotB contains an extracellular peptidoglycan-binding domain that anchors the complex to the cell wall and a transmembrane domain with a titratable aspartate residue that is protonated during consumption of the proton motive force (10, 11, 12). Protonation and deprotonation of MotB causes a conformational change in MotA, a multipass transmembrane protein with cytoplasmic loops critical for its function (9, 13, 14). Conformational changes in the cytoplasmic loop domains of MotA are thought to promote molecular contacts with the gear-like rotor of FliG and impart torque on the flagellum (14, 15, 16). Precisely how proton motive force consumption by MotB is converted into torque generation by MotA and FliG is still unclear, but many amino acids within these proteins have been identified both genetically and biochemically as being important for flagellar rotation (17, 18).

Flagellar rotation has been studied largely in the Gram-negative bacterium *Escherichia coli*, and here we characterize the conserved MotA and MotB flagellar stator proteins in the Gram-positive bacterium *Bacillus subtilis*. During the course of our study, we found that cells defective in the flagellar stator are not only nonmotile but also overproduce the secreted polymer poly-γ-glutamate (PGA) (19). In *B. subtilis*, PGA secretion results in the production of a mucoid slime layer, whereas in *Bacillus anthracis*, PGA is retained to the cell surface as a capsule (20, 21, 22). In both *B. subtilis* and *B. anthracis*, an operon of conserved biosynthetic genes (*pgsBCA* or *capABC* genes, respectively) is both necessary and sufficient for PGA synthesis (23, 24, 25, 26). In addition, *B. subtilis* encodes PgdS (also known as YwtD), which depolymerizes PGA (27, 28). Here, we show that a failure of proton conductance by the stator results in high-level synthesis and secretion of PGA, and we identify genetic determinants of PGA overproduction in strains with defective stators. Whereas some mutants that abolished PGA synthesis were defective in regulators of *pgs* expression, others were defective in flagellar filament assembly.

MATERIALS AND METHODS

Strains and growth conditions. *B. subtilis* strains were grown in Luria-Bertani (LB) (10 g tryptone, 5 g yeast extract, 5 g NaCl per liter) broth or on LB plates fortified with 1.5% Bacto agar at 37°C. When appropriate, antibiotics were included at the following concentrations: 10 μg/ml tetracycline, 100 μg/ml spectinomycin, 5 μg/ml chloramphenicol, 5 μg/ml kanamycin, and 1 μg/ml erythromycin plus 25 μg/ml lincomycin (mls). Isopropyl β-D-thiogalactopyranoside (IPTG; Sigma) was added to the medium at the indicated concentration when appropriate.

Swarm expansion assay. Cells were grown to mid-log phase at 37°C in LB broth and resuspended to an optical density at 600 nm (OD_{600}) of 10 in phosphate-buffered saline (PBS) buffer (137 mM NaCl, 2.7 mM KCl, 10 mM Na_2HPO_4, and 2 mM KH_2PO_4, pH 8.0) containing 0.5% India ink (Higgins). Freshly prepared LB containing 0.7% Bacto agar (25 ml/plate) was dried for 20 min in a laminar-flow hood, centrally inoculated with 10 μl of the cell suspension, dried for another 10 min, and incubated at 37°C. The India ink demarks the origin of the colony, and the swarm radius was measured relative to the origin. For consistency, an axis was drawn on the

Received 11 October 2013 **Accepted** 25 November 2013

Published ahead of print 2 December 2013

Address correspondence to Daniel B. Kearns, dbkearns@indiana.edu.

Supplemental material for this article may be found at http://dx.doi.org/10.1128/JB.01217-13.

doi:10.1128/JB.01217-13

back of the plate and swarm radii measurements were taken along this transect.

Colony images. Images were taken with a Leica EZ4D dissecting scope at 8× zoom.

Transposon mutagenesis. To generate mutants of the Δ*motA* strain that lost the mucoid colony morphology, the pMarA plasmid was introduced into strain DS7498 by SPP1 phage transduction (29). Mutagenesis was performed on each isolate by growing cells in 2 ml LB broth supplemented with kanamycin at 22°C for 24 h. Cells were diluted serially to 10^{-2}, 10^{-3}, and 10^{-4}, and 100 μl of each dilution was plated on prewarmed LB plates fortified with 1.5% agar supplemented with kanamycin and grown at the nonpermissive temperature (42°C) overnight. Colonies that were flat or had wild-type colony morphology were restreaked onto LB plates supplemented with kanamycin to verify the colony morphology. To confirm that the transposon was linked to the suppressor mutation, a lysate was generated on the mutant and the transposon was transduced to the parent strain (*motA* DS7498).

Inverse PCR. Chromosomal DNA was isolated from each mutant, and 1 μg of chromosomal DNA was digested with Sau3AI for 1 h. The digestion was then heat inactivated for 20 min, and 0.1 μg of digested DNA was ligated using T4 DNA ligase at room temperature for 1 h. PCR was conducted using each of the ligation reaction mixtures as a template, primers 695/696, and Phusion polymerase (New England BioLabs). Each PCR was column purified (Qiagen PCR extraction kit) and sequenced using primer 696. The sequence CCAACCTGT marks the end of the Mariner transposon insertion sequence. The next two bases are TA, according to the mechanism of mariner transposition, and mark the beginning of the chromosomal DNA specific to the insertion site (adapted from Pozsgai et al. [114]).

β-Galactosidase assay. Since PGA production and *pgs* operon expression are improved at high cell density, cells were harvested at an OD_{600} of approximately 1.5 (early stationary phase) to obtain β-galactosidase readings (30). One ml of cells was harvested from cultures at an OD_{600} of 1.5 and grown in LB broth at 37°C. Cells were resuspended in an equal volume of Z-buffer (40 mM NaH_2PO_4, 60 mM Na_2HPO_4, 1 mM $MgSO_4$, 10 mM KCl, and 38 mM 2-mercaptoethanol). To lyse cells, lysozyme was added to each sample to a final concentration of 0.2 mg ml^{-1} and incubated at 30°C for 15 min. Each sample was then diluted in Z-buffer to a final volume of 500 μl, and the reaction was started with 100 μl of 4 mg ml^{-1} 2-nitrophenyl β-D-galactopyranoside (in Z-buffer) and stopped with 250 μl of 1 M Na_2CO_3. The OD_{420} of the reaction mixture was measured, and β-galactosidase-specific activity was calculated using the equation $[OD_{420}/(\text{time} \times OD_{600})] \times \text{dilution factor} \times 1{,}000$.

Strain construction. All constructs were first introduced into the domesticated strain DS2569 by natural competence and then transferred to the 3610 background using SPP1-mediated generalized phage transduction (31). All strains used in this study are listed in Table 1. All plasmids used in this study are listed in Table S1 in the supplemental material. All primers used in this study are listed in Table S2.

In-frame deletions. To generate the Δ*motA* in-frame markerless deletion construct, the region upstream of *motA* was PCR amplified using the primer pair 2401/2402 and digested with EcoRI and XhoI, and the region downstream of *motA* was PCR amplified using the primer pair 2403/2404 and digested with XhoI and BamHI. The two fragments were then simultaneously ligated into the EcoRI and BamHI sites of pMiniMAD, which carries a temperature-sensitive origin of replication and an erythromycin resistance cassette to generate pEC1 (32). The plasmid pEC1 was introduced to DS2569 by single crossover integration by transformation at the restrictive temperature for plasmid replication (37°C) using mls resistance as a selection. The integrated plasmid was then transduced into 3610. To evict the plasmid, the strain was incubated in 3 ml LB broth at a permissive temperature for plasmid replication (22°C) for 14 h, diluted 30-fold in fresh LB broth, and incubated at 22°C for another 8 h. Dilution and outgrowth was repeated 2 more times. Cells were then serially diluted and plated on LB agar at 37°C. Individual colonies were patched on LB plates and LB plates containing mls to identify mls-sensitive colonies that had evicted the plasmid. Colony PCR was used on mls-sensitive colonies using primer pair 2401/2404 to determine which colony retained the Δ*motA* allele.

To generate pEC13 (Δ*mfd*), the region upstream of *mfd* was PCR amplified using the primer pair 2840/2841 and digested with EcoRI and BamHI, and the region downstream of *mfd* was PCR amplified using the primer pair 2842/2843 and digested with BamHI and SalI. The two fragments were then simultaneously ligated into the EcoRI/SalI sites of pMiniMAD. pEC13 was integrated into the *B. subtilis* DS2569 genome, transduced to strain 3610, and evicted as described above. Colonies were screened by PCR using primers 2840/2843 to determine which isolate had retained the Δ*mfd* allele.

To generate pEC14 (Δ*comQ*), the region upstream of *comQ* was PCR amplified using the primer pair 2844/2845 and digested with EcoRI and BamHI, and the region downstream of *comQ* was PCR amplified using the primer pair 2846/2847 and digested with BamHI and SalI. The two fragments were then simultaneously ligated into the EcoRI/SalI sites of pMiniMAD. pEC14 was integrated into the *B. subtilis* DS2569 genome, transduced to strain 3610, and evicted as described above. Colonies were screened by PCR using primers 2844/2847 to determine which isolate had retained the Δ*comQ* allele.

To generate pEC15 (Δ*flgL*), the region upstream of *flgL* was PCR amplified using the primer pair 2848/2849 and digested with KpnI and SalI, and the region downstream of *flgL* was PCR amplified using the primer pair 2850/2851 and digested with SalI and BamHI. The two fragments were then simultaneously ligated into the KpnI/BamHI sites of pMiniMAD. pEC15 was integrated into the *B. subtilis* PY79 genome, transduced to strain 3610, and evicted as described above. Colonies were screened by PCR using primers 2848/2851 to determine which isolate had retained the Δ*flgL* allele.

To generate pEC25 (Δ*pgsB*), the region upstream of *pgsB* was PCR amplified using the primer pair 3043/3001 and digested with BamHI and XhoI, and the region downstream of *pgsB* was PCR amplified using the primer pair 3002/3003 and digested with XhoI and EcoRI. The two fragments were then simultaneously ligated into the EcoRI/BamHI sites of pMiniMAD. pEC25 was integrated into the *B. subtilis* DS2569 genome, transduced to strain 3610, and evicted as described above. Colonies were screened by PCR using primers 3043/3003 to determine which isolate had retained the Δ*pgsB* allele.

To generate pEC32 (Δ*comX*), the region upstream of *comX* was PCR amplified using the primer pair 3126/3127 and digested with EcoRI and XhoI, and the region downstream of *comX* was PCR amplified using the primer pair 3128/3129 and digested with XhoI and BamHI. The two fragments were then simultaneously ligated into the EcoRI/BamHI sites of pMiniMAD. pEC32 was integrated into the *B. subtilis* DS2569 genome, transduced to strain 3610, and evicted as described above. Colonies were screened by PCR using primers 3126/3129 to determine which isolate had retained the Δ*comX* allele.

To generate pEC33 (Δ*comP*), the region upstream of *comP* was PCR amplified using the primer pair 3130/3131 and digested with EcoRI and XhoI, and the region downstream of *comP* was PCR amplified using the primer pair 3132/3133 and digested with XhoI and BamHI. The two fragments were then simultaneously ligated into the EcoRI/BamHI sites of pMiniMAD. pEC33 was integrated into the *B. subtilis* DS2569 genome, transduced to strain 3610, and evicted as described above. Colonies were screened by PCR using primers 3130/3133 to determine which isolate had retained the Δ*comX* allele.

To generate pDP374 (Δ*fliT*), the region upstream of *fliT* was PCR amplified using the primer pair 2641/2642 and digested with EcoRI and XhoI, and the region downstream of *fliT* was PCR amplified using the primer pair 2547/2548 and digested with XhoI and BamHI. The two fragments were then simultaneously ligated into the EcoRI/BamHI sites of pMiniMAD. pDP374 was integrated into the *B. subtilis* DS2569 genome, transduced to strain 3610, and evicted as described above. Colonies were

TABLE 1 Strains

Strain	Description[a]
3610	Wild type
DK1273	Δ*motA amyE*::$P_{hyspank}$-*motAmotB spec*
DK1318	Δ*motA bslA*::*kan*
DK1321	Δ*motA* Δ*fliD epsH*::*tet*
DK1322	Δ*motA* Δ*fliT epsH*::*tet*
DK1323	Δ*motA* Δ*degU epsH*::*tet*
DK1324	Δ*motA codY*::TnYLB *kan epsH*::*tet*
DK1325	Δ*motA* Δ*mfd epsH*::*tet*
DK1326	Δ*motA* Δ*comQ epsH*::*tet*
DK1328	Δ*motA* Δ*comP epsH*::*tet*
DK1329	Δ*motA* Δ*comX epsH*::*tet*
DK1330	Δ*motA* Δ*flgL epsH*::*tet*
DK1332	Δ*motA* Δ*pgsB epsH*::*tet*
DK1349	Δ*sigD epsH*::*tet*
DK1350	Δ*sigD epsH*::*tet amyE*::$P_{hyspank}$-*motA motB spec*
DK1351	Δ*fliF epsH*::*tet*
DK1352	Δ*fliF epsH*::*tet amyE*::$P_{hyspank}$-*motA motB spec*
DK1353	Δ*fliG epsH*::*tet*
DK1354	Δ*fliG epsH*::*tet amyE*::$P_{hyspank}$-*motA motB spec*
DK1360	Δ*motA epsH*::*tet*
DK1484	*srfAA*::*mls* Δ*epsH*
DK1492	*motAB*::*tet srfAA*::*mls* Δ*epsH*
DK1493	*motPS*::*tet srfAA*::*mls* Δ*epsH*
DK1558	Δ*motA* Δ*degS*
DK1572	Δ*motA* Δ*sigD pgsE*Ω*lacZ cat*
DK1573	Δ*motA* Δ*degS pgsE*Ω*lacZ cat*
DK1574	Δ*motA* Δ*sigD amyE*::P_{pgdS}-*lacZ cat*
DK1575	Δ*motA* Δ*degS amyE*::P_{pgdS}-*lacZ cat*
DK1578	Δ*motA* Δ*degS amyE*::$P_{hyspank}$-*degQ spec*
DK1579	Δ*motA* Δ*degS epsH*::*tet*
DS222	*motAB*::*tet*
DS223	*motPS*::*tet*
DS2569	Strain 3610 cured of pBS32 (115)
DS6420	Δ*sigD* (116)
DS7080	Δ*fliF*
DS7357	Δ*fliG*
DS7498	Δ*motA*
DS7548	Δ*motA* pMarA *TnYLB kan himar1 oriBS*(Ts) *kan mls*
DS7584	Δ*motB*
DS7617	Δ*motB amyE*::P_{motA}-*motA motB spec*
DS7624	Δ*motA amyE*::P_{motA}-*motA motB spec*
DS7753	Δ*motA fliT*ΩTnYLB *kan* (TATAAGGGT)
DS7755	Δ*motA fliD*ΩTnYLB *kan* (TAGCTGTCA)
DS7953	Δ*motB amyE*::P_{motA}-*motA* $motB^{D24N}$ *spec*
DS8088	Δ*motA pgsB*ΩTn*10 spec*
DS8122	Δ*motA fliD*ΩTnYLB *kan* (TACTAGCTC)
DS8123	Δ*motA tasA*ΩTn*10 spec*
DS8158	Δ*motB amyE*::P_{motA}-*motA* $motB^{D24E}$ *spec*
DS8276	Δ*motA* Δ*fliT*
DS8277	Δ*motA* Δ*fliD*
DS8367	Δ*motB amyE*::P_{motA}-*motA* $motB^{N24D}$ *spec* motile suppressor (revertant)
DS8368	Δ*motB amyE*::P_{motA}-*motA* $motB^{E24D}$ *spec* motile suppressor (pseudorevertant)
DS8369	Δ*motB amyE*::P_{motA}-*motA* $motB^{E24D}$ *spec* motile suppressor (pseudorevertant)
DS8410	Δ*motA epsH*::*tet*
DS8428	Δ*motA srfAA*::*mls*
DS8572	Δ*motA fliT*ΩTnYLB *kan* (TAATATGTG)
DS8573	Δ*motA flgL*ΩTnYLB *kan* (TAACTGCTT)
DS8574	Δ*motA fliD*ΩTnYLB *kan* (TATAGTCTC)
DS8644	Δ*sigD amyE*::$P_{hyspank}$-*motA motB spec*
DS8654	Δ*motA comP*ΩTnYLB *kan* (TATATGCTA)

TABLE 1 (Continued)

Strain	Description[a]
DS8656	Δ*motA mfd*ΩTnYLB *kan* (TAATCTCCA)
DS8657	Δ*motA pgsB*ΩTnYLB *kan* (TACTCATCT)
DS8689	Δ*motA degS*ΩTnYLB *kan* (TACTTGAAT)
DS8691	Δ*motA mfd*ΩTnYLB *kan* (TAACTCTGT)
DS8701	Δ*motA* <*degU*ΩTnYLB *kan* (TATATAGAA)
DS8913	Δ*motA* Δ*degU*
DS8935	Δ*motA mfd*ΩTnYLB *kan* (TAAGGGTCT)
DS8936	Δ*motA comP*ΩTnYLB *kan* (TATATATGC)
DS8938	Δ*motA mfd*ΩTnYLB *kan* (TAGCATAAC)
DS8939	Δ*motA fliD*ΩTnYLB *kan* (TACGATATC)
DS8940	Δ*motA mfd*ΩTnYLB *kan* (TATCAATTT)
DS8968	Δ*motA pgsE*Ω*lacZ cat*
DS8971	Δ*motA comX*ΩTnYLB *kan* (TATAAGGCA)
DS8972	Δ*motA comP*ΩTnYLB *kan* (TAAAAAATC)
DS8985	Δ*motA mfd*ΩTnYLB *kan* (TAATCGCTG)
DS9018	Δ*motA codY*ΩTnYLB *kan* (TAGATTTTC)
DS9019	Δ*motA degS*ΩTnYLB *kan* (TACAGTCAA)
DS9020	Δ*motA comQ*ΩTnYLB *kan* (TATCCCCCT)
DS9021	Δ*motA degU*ΩTnYLB *kan* (TAACCTCTC)
DS9022	Δ*motA* <*comQ*ΩTnYLB *kan* (TATCTGCTC)
DS9061	Δ*motA* Δ*mfd*
DS9062	Δ*motA* Δ*flgL*
DS9078	Δ*motA* Δ*comQ*
DS9079	*pgsE*Ω*lacZ cat*
DS9134	Δ*motA codY*::TnYLB *kan pgsE*Ω*lacZ cat*
DS9246	Δ*motA amyE*::P_{motA}-$motA^{P155T}$ *motB spec*
DS9259	*epsH*::*tet*
DS9278	Δ*motA amyE*::P_{motA}-$motA^{P155R}$ *motB spec*
DS9280	Δ*motA amyE*::P_{motA}-$motA^{R90H}$ *motB spec*
DS9309	*amyE*::P_{pgdS}-*lacZ cat*
DS9310	*amyE*::$P_{hyspank}$-*degQ spec*
DS9349	Δ*motA amyE*::P_{pgdS}-*lacZ cat*
DS9350	Δ*motA amyE*::$P_{hyspank}$-*degQ spec*
DS9382	Δ*motA comP*ΩTnYLB *kan* (TATTAAAAA)
DS9383	Δ*motA comP*ΩTnYLB *kan* (TATAAAGGA)
DS9453	Δ*motA codY*ΩTnYLB *kan amyE*::P_{pgdS}-*lacZ cat*
DS9459	Δ*motA codY*ΩTnYLB *kan amyE*::$P_{hyspank}$-*degQ spec*
DS9575	Δ*motA amyE*::P_{motA}-$motA^{R90G}$ *motB spec*
DS9606	Δ*motA amyE*::P_{motA}-$motA^{P203R}$ *motB spec*
DS9627	Δ*motA flgL*ΩTnYLB *kan* (TAAGTTCCG)
DS9628	Δ*motA* Δ*pgsB*
DS9691	Δ*motA* Δ*fliD pgsE*Ω*lacZ cat*
DS9692	Δ*motA* Δ*fliT pgsE*Ω*lacZ cat*
DS9693	Δ*motA* Δ*comQ pgsE*Ω*lacZ cat*
DS9695	Δ*motA* Δ*degU pgsE*Ω*lacZ cat*
DS9696	Δ*motA* Δ*mfd pgsE*Ω*lacZ cat*
DS9699	Δ*motA* Δ*fliD amyE*::P_{pgdS}-*lacZ cat*
DS9700	Δ*motA* Δ*fliT amyE*::P_{pgdS}-*lacZ cat*
DS9701	Δ*motA* Δ*comQ amyE*::P_{pgdS}-*lacZ cat*
DS9703	Δ*motA* Δ*degU amyE*::P_{pgdS}-*lacZ cat*
DS9704	Δ*motA* Δ*mfd amyE*::P_{pgdS}-*lacZ cat*
DS9707	Δ*motA* Δ*fliD amyE*::$P_{hyspank}$-*degQ spec*
DS9708	Δ*motA* Δ*fliT amyE*::$P_{hyspank}$-*degQ spec*
DS9709	Δ*motA* Δ*comQ amyE*::$P_{hyspank}$-*degQ spec*
DS9711	Δ*motA* Δ*degU amyE*::$P_{hyspank}$-*degQ spec*
DS9712	Δ*motA* Δ*mfd amyE*::$P_{hyspank}$-*degQ spec*
DS9735	Δ*motA* Δ*flgL pgsE*Ω*lacZ cat*
DS9736	Δ*motA* Δ*flgL amyE*::P_{pgdS}-*lacZ cat*
DS9737	Δ*motA* Δ*flgL amyE*::$P_{hyspank}$-*degQ spec*
DS9738	Δ*motA* Δ*pgsB pgsE*Ω*lacZ cat*
DS9739	Δ*motA* Δ*pgsB amyE*::P_{pgdS}-*lacZ cat*
DS9740	Δ*motA* Δ*pgsB amyE*::$P_{hyspank}$-*degQ spec*

(Continued on following page)

TABLE 1 (Continued)

Strain	Description[a]
DS9763	Δ*motA amyE*::P_{motA}-*motA*^{P203T}*motB spec*
DS9796	Δ*motA* Δ*comX*
DS9797	Δ*motA* Δ*comP*
DS9802	Δ*motA amyE*::P_{motA}-*motA*^{H90R}*motB spec* motile suppressor (revertant)
DS9803	Δ*motA amyE*::P_{motA}-*motA*^{H90R}*motB spec* motile suppressor (revertant)
DS9804	Δ*motA amyE*::P_{motA}-*motA*^{H90R}*motB spec* motile suppressor (revertant)
DS9809	Δ*motA* Δ*comX pgsE*Ω*lacZ cat*
DS9810	Δ*motA* Δ*comP pgsE*Ω*lacZ cat*
DS9811	Δ*motA* Δ*comX amyE*::P_{pgdS}-*lacZ cat*
DS9812	Δ*motA* Δ*comP amyE*::P_{pgdS}-*lacZ cat*
DS9813	Δ*motA* Δ*comX amyE*::$P_{hyspank}$-*degQ spec*
DS9814	Δ*motA* Δ*comP amyE*::$P_{hyspank}$-*degQ spec*
DS9874	Δ*fliG amyE*::$P_{hyspank}$-*motAmotB spec*
DS9875	Δ*fliF amyE*::$P_{hyspank}$-*motAmotB spec*
DS9877	Δ*motA amyE*::P_{motA}-*motA*^{R155P}*motB spec* motile suppressor (revertant)

[a] <, Insertion is upstream of the indicated gene. DNA sequence in parentheses indicates the sequence of 9 bp of host DNA immediately adjacent to the transposon to permit identification of the precise location of each insertion.

screened by PCR using primers 2641/2548 to determine which isolate had retained the Δ*fliT* allele.

To generate pMP196 (Δ*degS*), the region upstream of *degS* was PCR amplified using the primer pair 3899/3900 and digested with BamHI and NotI, and the region downstream of *degS* was PCR amplified using the primer pair 3901/3902 and digested with NotI and SalI. The two fragments were then simultaneously ligated into the BamHI/SalI sites of pMiniMAD. pMP196 was integrated into the *B. subtilis* DS2569 genome, transduced to strain 3610, and evicted as described above. Colonies were screened by PCR using primers 3899/3902 to determine which isolate had retained the Δ*degS* allele.

Complementation constructs. To generate the P_{motA}-*motA motB* complementation construct pEC6, a PCR product containing the *motA motB* coding region plus 500 bp of upstream sequence was amplified from *B. subtilis* 3610 chromosomal DNA using the primer pair 2471/2472, digested with BamHI and SalI, and cloned into the BamHI and SalI sites of pAH25 containing a polylinker and spectinomycin resistance cassette between two arms of the *amyE* (35).

Inducible constructs. To generate the $P_{hyspank}$-*motA motB* construct pEC10, a PCR product containing *motA motB* was amplified from 3610 chromosomal DNA using the primer pair 2773/2774, digested with SalI and NheI, and cloned into the SalI and NheI sites of pDR111 containing a spectinomycin resistance cassette, a polylinker downstream of the $P_{hyspank}$ promoter, and the gene encoding the LacI repressor between the two arms of the *amyE* gene (33). The $P_{hyspank}$-*degQ* construct (pEC20) was built similarly using primer pair 2957/2958.

Site-directed mutagenesis. To generate the P_{motA}-*motA motB*^{D24N} allele complementation construct pEC7, site-directed mutagenesis was performed using the QuikChange II kit (Stratagene) on pEC6, using the primer pair 2571/2572 to change codon 24 of *motB* from GAC (aspartate) to AAC (asparagine). The P_{motA}-*motA motB*^{D24E} allele complementation construct pEC8 was built similarly using the primer pair 2630/2631 to change codon 24 of *motB* from GAC (aspartate) to GAG (glutamate). Sequences were verified by sequencing with primers 1008/2623.

The P_{motA}-*motA*^{R90H} *motB* allele complementation construct pEC18 was built similarly using the primer pair 2914/2915 to change codon 90 of *motA* from CGC (arginine) to CAC (histidine). The P_{motA}-*motA*^{R90G} *motB* allele complementation construct pEC24 was built similarly using the primer pair 3008/3009 to change codon 90 of *motA* from CGC (arginine) to GGC (glycine). The P_{motA}-*motA*^{P155T} *motB* allele complementation construct pEC16 was generated similarly through site-directed mutagenesis of pEC6 using the primer pair 2918/2919 to change codon 155 of *motA* from CCG (proline) to ACG (threonine). The P_{motA}-*motA*^{P155R} *motB* allele complementation construct pEC17 was built similarly using the primer pair 2916/2917 to change codon 155 of *motA* from CCG (proline) to CGG (arginine). The P_{motA}-*motA*^{P203T} *motB* allele complementation construct pEC30 was built similarly using the primer pair 3012/3013 to change codon 203 of *motA* from CCT (proline) to ACT (threonine). The P_{motA}-*motA*^{P203R} *motB* allele complementation construct pEC27 was built similarly using the primer pair 3010/3011 to change codon 203 of *motA* from CCT (proline) to CGT (arginine). Sequences were verified by sequencing with primers 822/823/2465.

LacZ reporter constructs. To generate the β-galactosidase (*lacZ*) reporter construct pEC12, a 613-bp PCR product from the last gene of the *pgs* operon (*pgsE*) was amplified using *B. subtilis* 3610 chromosomal DNA with primers 2811/2812. The PCR product was digested with EcoRI and BamHI and cloned into the EcoRI and BamHI sites of plasmid pEX44, which carries a chloramphenicol resistance marker and a polylinker upstream of the *lacZ* gene (generous gift from Patrick Eichenberger).

To generate the β-galactosidase (*lacZ*) reporter construct pEC19, PCR product from the P_{pgdS} promoter was amplified using *B. subtilis* 3610 chromosomal DNA with primers 2955/2956. The PCR product was digested with EcoRI and BamHI and cloned into the EcoRI and BamHI sites of plasmid pDG268, which carries a chloramphenicol resistance marker and a polylinker upstream of the *lacZ* gene between two arms of the *amyE* gene (34).

Allelic replacement. The Δ*motPS*::*tet* insertion deletion allele was generated by long flanking homology PCR (using primers 93/94 and 95/96), and DNA containing a tetracycline drug resistance gene (pDG1515) was used as a template for marker replacement (35, 36).

The Δ*bslA*::*spec* insertion deletion allele was generated by long flanking homology PCR (using primers 1535/1536 and 1537/1538), and DNA containing a spectinomycin drug resistance gene (pAH54) was used as a template for marker replacement.

SPP1 phage transduction. To 0.2 ml of dense culture grown in TY broth (LB broth supplemented after autoclaving with 10 mM $MgSO_4$ and 100 μM $MnSO_4$), serial dilutions of SPP1 phage stock were added and statically incubated for 15 min at 37°C. To each mixture, 3 ml TYSA (molten TY supplemented with 0.5% agar) was added, poured atop fresh TY plates, and incubated at 37°C overnight. Top agar from the plate containing nearly confluent plaques was harvested by scraping into a 50-ml conical tube, vortexed, and centrifuged at 5,000 × *g* for 10 min. The supernatant was treated with a final concentration of 25 μg/ml DNase I before being passed through a 0.45-μm syringe filter and stored at 4°C.

Recipient cells were grown to stationary phase in 2 ml TY broth at 37°C. Cells (0.9 ml) were mixed with 5 μl of SPP1 donor phage stock. Nine ml of TY broth was added to the mixture and allowed to stand at 37°C for 30 min. The transduction mixture was then centrifuged at 5,000 × *g* for 10 min, the supernatant was discarded, and the pellet was resuspended in the remaining volume. One hundred μl of cell suspension was then plated on TY fortified with 1.5% agar, the appropriate antibiotic, and 10 mM sodium citrate.

RESULTS

MotA and MotB are required for motility. The *B. subtilis* genome contains two sets of cooriented dicistrons encoding protein pairs MotA/MotB and MotP/MotS, which are homologous to those that encode the flagellar stator of *E. coli* (Fig. 1A). Although MotA/MotB has been shown to be required for swimming motility of domesticated laboratory strains, some bacteria encode multiple stator complexes specifically dedicated to swarming over surfaces (37, 38, 39, 40, 41). To determine if one or both stator homologs were required for motility of the ancestral strain of *B. subtilis*, antibiotic marker replacement mutations were generated for each

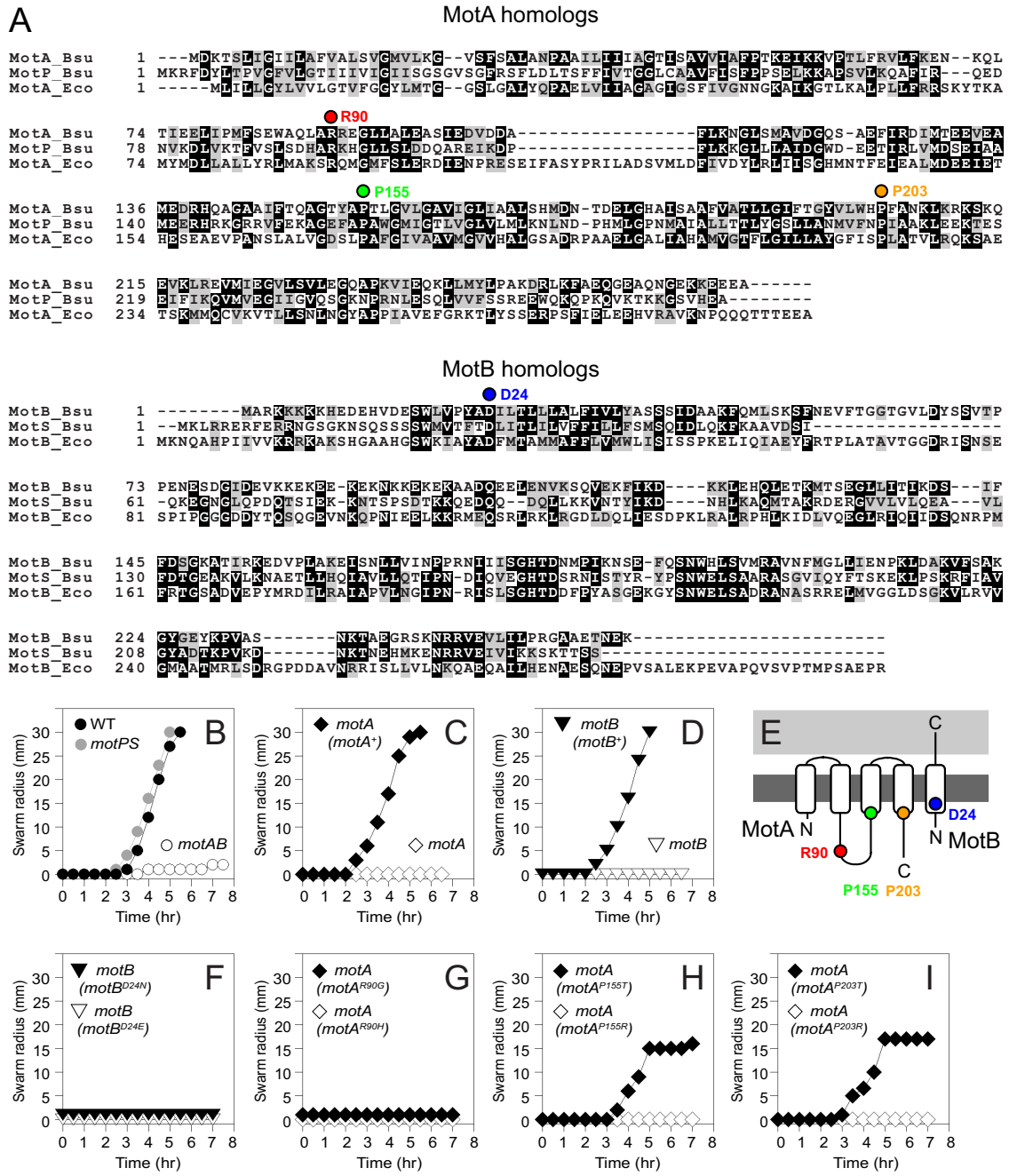

FIG 1 MotA and MotB residues required for motility. (A) Multiple sequence alignments of MotA/MotP proteins and MotB/MotS proteins from *B. subtilis* (Bsu) and *E. coli* (Eco). Colored circles above residues indicate residues drawn in the cartoon of panel E and mutated in panels F to I. (B) Swarm expansion assay of wild-type (3610; closed circles), *motAB* (DS222; open circles), and *motPS* (DS223; gray circles) strains. (C) Swarm expansion assay of *motA* (DS7498; open symbols) and the *motA* (*motA*$^{+}$) complemented strain (DS7624; closed symbols). (D) Swarm expansion assay of *motB* (DS7584; open symbols) and the *motB* (*motB*$^{+}$) complemented strain (DS7617; closed symbols). (E) Cartoon of MotA and MotB proteins inserted in the membrane (dark gray) and peptidoglycan (light gray). The relative positions of residues mutated by site-directed mutation are indicated by colored circles that correspond to their location in the primary sequence shown in panel A. N termini and C termini are indicated by "N" and "C," respectively. (F) Swarm expansion assay of *motB* (*motB*^{D24N}) (DS7953; closed symbols) and *motB* (*motB*^{D24E}) (DS8158; open symbols) strains. (G) Swarm expansion assay of *motA* (*motA*^{R90G}) (DS9575; closed symbols) and *motA* (*motA*^{R90H}) (DS9280; open symbols) strains. (H) Swarm expansion assay of *motA* (*motA*^{P155T}) (DS9246; closed symbols) and *motA* (*motA*^{P155R}) (DS9278; open symbols) strains. (I) Swarm expansion assay of *motA* (*motA*^{P203T}) (DS9763; closed symbols) and *motA* (*motA*^{P203R}) (DS9606; open symbols) strains. For swarming motility assays, all points are averages from three replicates.

pair. Whereas strains that lacked *motP* and *motS* exhibited swimming and swarming like the wild type, strains that lacked *motA* and *motB* were abolished for both forms of motility (Fig. 1B; also see Fig. S1 in the supplemental material). Prolonged incubation of the *motAB* double mutant did not yield suppressor mutations that restored motility. We conclude that MotA and MotB are required for motility and that there are no redundant systems in *B. subtilis* that can compensate for their absence.

TABLE 2 Phenotypes and suppressors of MotA/MotB alleles

Gene	Allele	Phenotype	Suppressor(s)[a]
motB	D24N	Nonmotile	Revertant (DS8367)
motB	D24E	Nonmotile	Pseudorevertants (DS8368, DS8369)
motA	R90H	Nonmotile	Revertants (DS9802, DS9803, DS9804)
motA	R90G	Nonmotile	NR
motA	P155T	Reduced motility	NR
motA	P155R	Nonmotile	Revertant (DS9877)
motA	P203T	Reduced motility	NR
motA	P203R	Nonmotile	NR

[a] NR, none recovered.

Separate in-frame markerless deletion mutations of either *motA* or *motB* gave nonmotile phenotypes similar to that of the *motAB* double mutant (Fig. 1C and D). To confirm that loss of motility was a direct consequence of the loss of *motA* and *motB*, each mutant was complemented by incorporating a copy of the wild-type allele at an ectopic locus in the chromosome. Since *motA* and *motB* have overlapping reading frames, both genes were cloned downstream of the native promoter (P_{motA}) and inserted into the ectopic *amyE* site to generate the complementation construct (*amyE*::P_{motA}-*motAB*). Introduction of the P_{motA}-*motAB* complementation construct into either the *motA* or *motB* deletion mutant restored swarming motility to levels comparable to that of the wild type (Fig. 1C and D). We conclude that both MotA and MotB are required for *B. subtilis* motility and that loss-of-function mutations in either protein can be complemented when the corresponding gene is provided *in trans*.

MotA and MotB of *B. subtilis* contain conserved residues that are required for flagellar function in *E. coli* (Fig. 1A and E). In *E. coli* MotB, aspartate[32] is critical for interacting with a proton in the stator channel during energy transduction (11, 14). The corresponding residue in *B. subtilis*, aspartate[24] (D24), was mutated to either asparagine (D24N) or glutamate (D24E) in the complementation construct (*amyE*::P_{motA}-*motA motB*$^{D24N/E}$). Consistent with a requirement for aspartate[24], the mutated alleles of MotB^{D24N} or MotB^{D24E} failed to restore motility to a *motB* mutant (Fig. 1F). Prolonged incubation of these mutants, however, yielded three suppressor mutations that restored motility to levels comparable to that of the wild type. The suppressor of MotB^{D24N} was a direct revertant to the original aspartate codon (AAC>GAC), and two independently isolated suppressors of MotB^{D24E} were pseudorevertants that restored the aspartate residue via an alternative codon (GAG>GAT) (Table 2). We conclude that MotB residue aspartate[24] is required for MotB stability or function.

In *E. coli*, MotA residue arginine[90] (R90) interacts with the FliG rotor to generate flagellar rotation (17, 18). The corresponding residue in *B. subtilis* MotA, arginine[90], was mutated to either glycine (MotA^{R90G}) or histidine (MotA^{R90H}) in the complementation construct, and both mutations failed to restore motility to a *motA* mutant (Fig. 1G). Prolonged incubation of these mutants, however, yielded three suppressor mutations of MotA^{R90H} that restored motility to levels comparable to that of the wild type. All three suppressors were revertants to the original arginine codon (CGC>GAC) (Table 2). Suppressors were not obtained from the MotA^{R90G} allele. We conclude that MotA residue arginine[90] is required for MotA stability or function.

Two proline residues in *E. coli* MotA, proline[173] and proline[222], participate in a MotA conformational change thought to be required for interaction with FliG to generate torque (Fig. 1E) (14, 17, 18). Mutating proline[155] in *B. subtilis* MotA (corresponding to *E. coli* proline[173]) and proline[203] (corresponding to *E. coli* proline[222]) to arginine abolished swarming motility, but mutating either residue to threonine did not (Fig. 1H and I). Only one suppressor mutation was isolated from the alleles with mutated prolines, and MotA^{P155R} experienced a reversion (CGG>CCG) to the original proline codon (Table 2). Similar null and partial phenotypes were observed in *E. coli* when the conserved prolines were mutated to arginine and threonine, respectively (17). We conclude that proline[155] and proline[203] are required for either MotA stability or function. When one is mutated, it causes a severity of defect that depends on the residue to which the proline is mutated.

Mutation of the flagellar stator proteins increases PGA synthesis. While studying the motility phenotype of the motor protein mutants, we observed that the *motA* and *motB* mutants formed large, mucoid colonies (Fig. 2A). Often there appeared to be a dull-looking skin on top of the colony that obscured the mucoid material, but probing with a toothpick revealed extensive mucoidy underneath. Due to its viscous extracellular nature, we hypothesized that the mucoid material was the result of one or more of the following substances: extracellular polysaccharide (EPS), the lipopeptide surfactin, a secreted protein polymer, and/or poly-γ-glutamate (PGA). To determine the composition of the mucoid material, we combined mutations in *motA* with mutations in *epsH*, encoding an enzyme required for EPS production; *srfAA*, encoding an enzyme required for surfactin production; *tasA*, encoding an extracellular EPS-organizing protein; *bslA*, encoding a secreted hydrophobin; or *pgsB*, encoding an enzyme required for PGA production (25, 42, 43, 44, 45, 46, 47). The *motA tasA* and *motA srfAA* double mutants exhibited extensive mucoidy underneath a skin-like substance comparable to the *motA* single mutant (Fig. 2B). In contrast, the *motA epsH* and *motA bslA* mutants were highly mucoid but lacked the skin-like colony cover (Fig. 2B). Lastly, the *motA pgsB* double mutant that abolished PGA was nonmucoid (Fig. 2B). Our results are consistent with another recent report that demonstrated PGA-dependent mucoidy in flagellar stator mutants (48). We conclude that EPS and BslA were components of the surface skin and that PGA overproduction was responsible for mucoidy in the *mot* deletion mutants.

PGA overproduction was also observed in the MotA and MotB loss-of-function point mutant alleles. Cells mutated for the MotB proton-conducting aspartate residues, MotB^{D24N} and MotB^{D24E}, had mucoid colony morphology, whereas the MotB revertants both restored motility and abolished mucoidy (Fig. 2C). Similarly, the MotA^{R90H}, MotA^{P115R}, and MotA^{P203R} mutants both abolished motility and conferred mucoidy, whereas the MotA revertants retained motility and exhibited a nonmucoid colony morphology (Fig. 2D). Finally, the MotA^{P155T} and MotA^{P203T} mutants that retained motility also exhibited a nonmucoid colony morphology (Fig. 2D). Thus, each mutant that was severely defective in motility also resulted in PGA overproduction. We infer that the role of MotA and MotB in the regulation of PGA synthesis is dependent on their presence or function, being related either to proton flow, the conformational changes of the stator complex, or flagellar rotation.

PGA overproduction was also observed in mutants defective in flagellar basal body assembly, including mutations in the *fliF* gene,

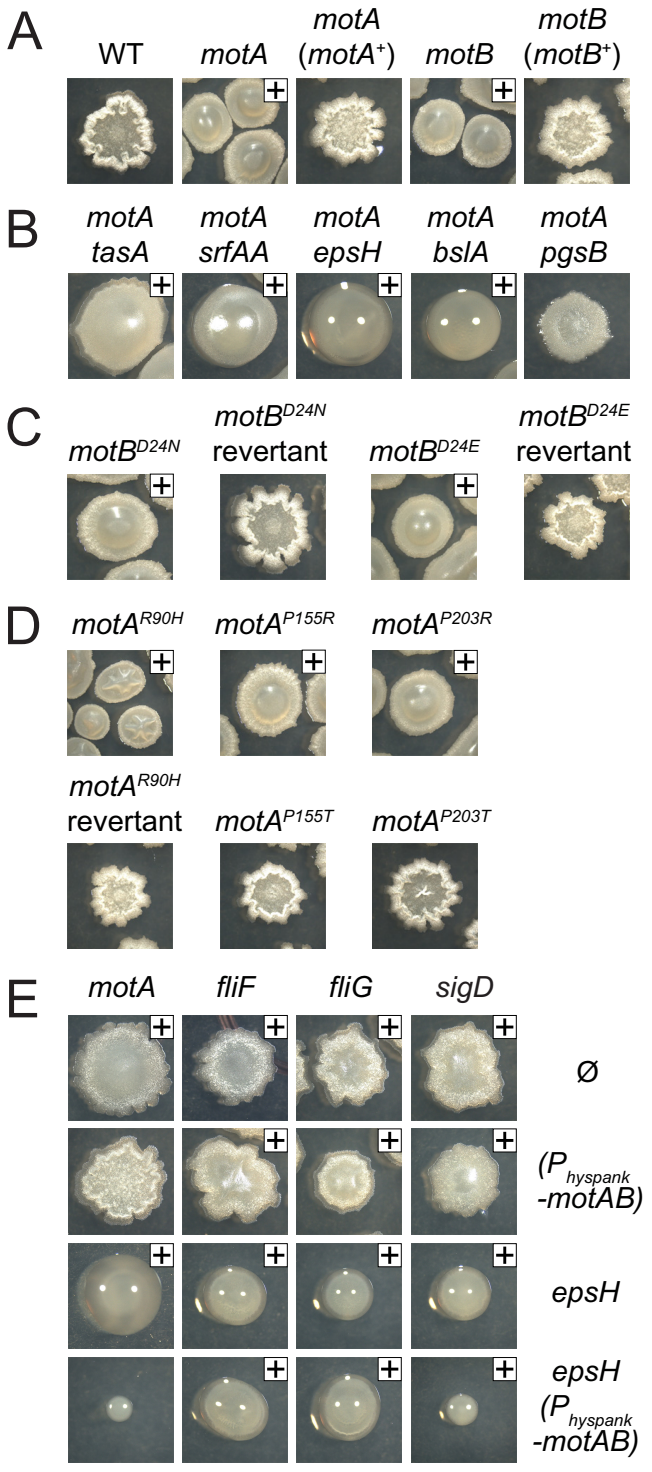

FIG 2 Cells defective for the flagellar motor create mucoid colonies. Top images are of cultures grown overnight at 37°C. A plus sign is included in the upper right corner to indicate our interpretation that the colony was mucoid. Sometimes, the mucoidy was concealed under a skin-like material and could be better observed when the colony was probed with a toothpick. The following strains were used to generate this figure: wild type (3610), *motA* (DS7498), *motA* (*motA*$^{+}$) (DS7624), *motB* (DS7584), *motB* (*motB*$^{+}$) (DS7617) (A); *motA tasA* (DS8123), *motA srfAA* (DS8428), *motA epsH* (DS8410), *motA bslA* (DK1318), *motA pgsB* (DS8088) (B); *motB* (*motB*^{D24N}) (DS7953), *motB* (*motB*^{N24D}) (DS8367), *motB* (*motB*^{D24E}) (DS8158), *motB* (*motB*^{E24D}) (DS8368) (C); *motA* (*motA*^{R90H}) (DS9280), *motA* (*motA*^{H90R}) (DS9802), *motA* (*motA*^{P155R}) (DS9278), *motA* (*motA*^{P155T}) (DS9246), *motA* (*motA*^{P203R}) (DS9606), and *motA* (*motA*^{P203T}) (DS9763) (D); *motA* (DS7498), *motA* $P_{hyspank}$-*motAB* (DK1273), *motA epsH* (DK1360), *motA epsH* $P_{hyspank}$-*motAB* (DK1361), *fliF* (DS7080), *fliF* $P_{hyspank}$-*motAB* (DS9875), *fliF epsH* (DK1351), *fliF epsH* $P_{hyspank}$-*motAB* (DK1352), *fliG* (DS7357), *fliG* $P_{hyspank}$-*motAB* (DS9874), *fliG epsH* (DK1353), *fliG epsH* $P_{hyspank}$-*motAB* (DK1354), *sigD* (DS6420), *sigD* $P_{hyspank}$-*motAB* (DS8644), *sigD epsH* (DK1349), and *sigD epsH* $P_{hyspank}$-*motAB* (DK1350) (E).

encoding the FliF basal body base protein, and the *fliG* gene, encoding the FliG rotor, which physically transduces force from MotA to the rotation of FliF (Fig. 2E). Mutations in *fliF* and *fliG* could confer a mucoid phenotype due to a failure to express *motA* and *motB*, because defects in basal body assembly result in inhibition of the σ^{D} alternative sigma factor that directs *motA* and *motB* transcription (37, 49). Consistent with a defect in *motA* and *motB* expression, mucoidy was also observed for an in-frame markerless deletion of the *sigD* gene, encoding σ^{D} (Fig. 2E). To test whether defects in *motA* and *motB* expression were sufficient to explain the mucoid phenotype of basal body mutants, the *motAB* operon was cloned downstream of the artificial IPTG-inducible $P_{hyspank}$ promoter and inserted at the ectopic *amyE* locus (*amyE*::$P_{hyspank}$-*motA motB*). Colony morphology assays were conducted in cells wild type for EpsH and cells mutated for *epsH* to remove the surface skin so that mucoidy could be more easily observed. Artificial induction of *motA* and *motB* by IPTG reduced mucoidy in the *motA* and *sigD* mutant backgrounds but did not reduce mucoidy in the *fliF* and *fliG* mutant backgrounds (Fig. 2E). We conclude that PGA overproduction results as a failure of stator conductance that can be caused by mutation of either the stator or the rotor components of the flagellar motor.

Transposon mutagenesis identifies regulators of PGA production in motor mutants. Flagella motor proteins have only recently been associated with PGA production, and the relationship between the two is neither evident nor well understood based on the genetic analysis thus far (48). To find regulators of PGA production, *mariner* transposon mutagenesis was conducted in a Δ*motA* mutant, and over 16,000 colonies were screened for a loss-of-mucoidy phenotype. Twenty-seven nonmucoid colonies were independently isolated, and all mutants were backcrossed using SPP1-mediated generalized transduction into the *motA* parent to ensure that the loss-of-mucoidy phenotype was inseparably linked to the transposon insertion. The location of each transposon insertion was identified (Fig. 3A). In-frame markerless deletions were generated in a *motA* background to further validate genes found to be disrupted by a transposon insertion (Fig. 3B). In addition, each mutant was also mutated for *epsH* to abolish the colony skin so that the presence or absence of mucoidy could be more easily observed (Fig. 3B). One of the 27 mutants directly disrupted PGA synthesis by an insertion in *pgsB* (TnΩDS*8657*), whereas the remaining 26 insertions were located outside the *pgs* operon and were organized into 3 conceptual classes (Table 3).

Class 1 transposon insertions that abolished mucoidy in a *motA* mutant disrupted genes involved in the biogenesis of the flagellar filament (Fig. 3 and Table 3). Four insertions disrupted *fliD*, encoding the FliD filament cap that serves as an extracytoplasmic chaperone required for polymerization of flagellin into the helical filament (50, 51, 52). Two insertions disrupted *fliT*, encoding FliT, a protein thought to act as a cytoplasmic chaperone for the secretion of FliD (53, 54). Two insertions disrupted *flgL*,

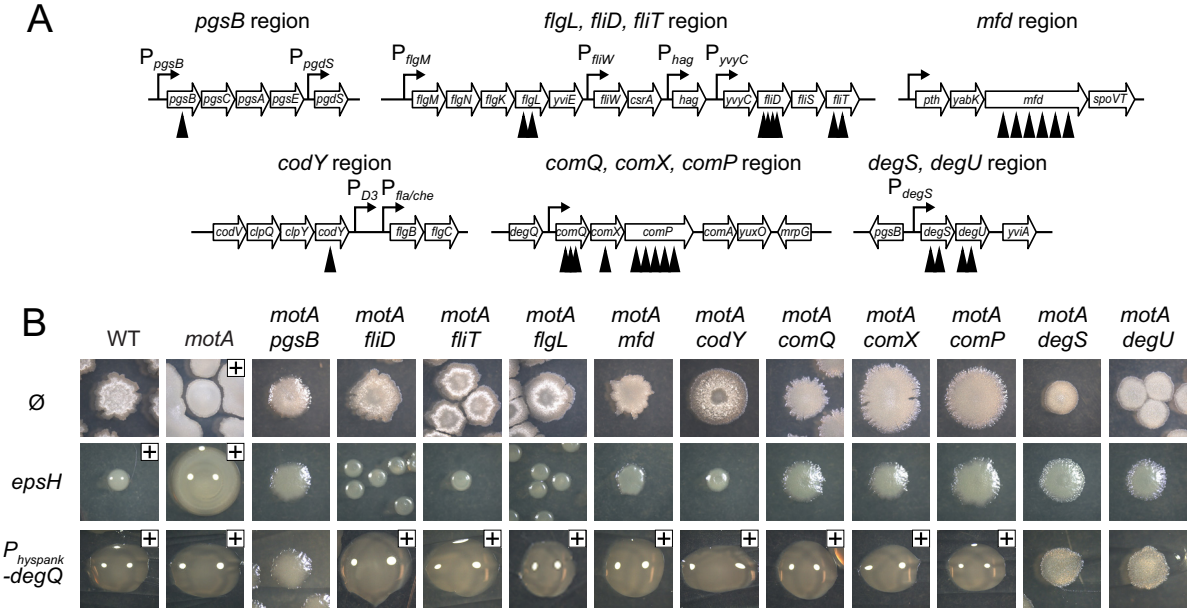

FIG 3 Location of genes which, when mutated, abolish mucoid colony morphology in a Δ*motA* mutant. (A) Gene maps depicting the location of transposon insertions that abolished mucoidy in a Δ*motA* background. Open arrows indicate open reading frames. Bent arrows indicate promoters. Black carets indicate the relative location of transposon insertions. Distances are not to scale. (B, row Ø) Colony images of the indicated genotype with no additional mutations: wild type (3610), *motA* (DS7498), *motA pgsB* (DS9628), *motA fliD* (DS8277), *motA fliT* (DS8276), *motA flgL* (DS9062), *motA mfd* (DS9061), *motA codY* (DS9018), *motA comQ* (DS9078), *motA comX* (DS9796), *motA comP* (DS9797), *motA degS* (DK1558), and *motA degU* (DS8913). (Row *epsH*) Colony images of the indicated genotype with an additional *epsH* mutation to abolish the colony skin and reveal the extent of mucoidy: wild type (DS9259), *motA* (DK1360), *motA pgsB* (DK1332), *motA fliD* (DK1321), *motA fliT* (DK1322), *motA flgL* (DK1330), *motA mfd* (DK1325), *motA codY* (DK1324), *motA comQ* (DK1326), *motA comX* (DK1329), *motA comP* (DK1328), *motA degS* (DK1579), and *motA degU* (DK1323). (Row $P_{hyspank}$-*degQ*) Colony images of the indicated genotype with an additional $P_{hyspank}$-*degQ* construct grown in the presence of 1 mM IPTG: wild type (DS9310), *motA* (DS9350), *motA pgsB* (DS9740), *motA fliD* (DS9707), *motA fliT* (DS9708), *motA flgL* (DS9737), *motA mfd* (DS9712), *motA codY* (DS9459), *motA comQ* (DS9709), *motA comX* (DS9813), *motA comP* (DS9814), *motA degS* (DK1578), and *motA degU* (DS9711).

encoding FlgL, a protein predicted to form the hook-filament junction upon which the FliD cap is assembled in *Salmonella enterica* (55, 56, 57). Thus, the class 1 mutants appeared to be related to FliD, in that FliD itself was disrupted and FliT and FlgL are required for FliD secretion and assembly, respectively.

Six class 2 transposon insertions disrupted the gene *mfd*, encoding Mfd, a protein involved in transcription-coupled DNA repair, the process by which lesions are repaired on the template strand of expressed genes at a higher frequency than lesions on the coding strand of the same gene (Fig. 3 and Table 3) (58–62). Mfd interacts with RNA polymerase stalled at a damaged base, dissociates RNA polymerase from the DNA template, and recruits the DNA excision repair complex (63–66). Recently, Mfd was also found to release RNA polymerase when stalled by a head-on collision with DNA polymerase in the replication fork (67, 68). Finally, in *B. subtilis* Mfd has been shown to play a regulatory role by resolving RNA polymerase stalled at *cis* elements, including high-affinity binding sites for DNA binding repressor proteins (69, 70). How Mfd increases PGA synthesis in the absence of MotA/MotB is unknown; however, we infer that the resolution of stalled RNA polymerase by Mfd plays a role.

Class 3 transposon insertions disrupted genes involved in transcriptional gene regulation (Fig. 3 and Table 3). One transposon insertion disrupted *codY*, encoding CodY, a pleiotropic transcriptional repressor that represses genes required for stationary phase and sporulation (71, 72, 73). Eight transposon insertions disrupted the ComQXP quorum-sensing regulatory system involved in cell density-dependent induction of genes required for surfactant biosynthesis and genes required for natural competence (74, 75). The secreted ComX pheromone peptide is modified by ComQ and detected by the ComP two-component histidine kinase and cognate ComA response regulator (76–79). Finally, four transposon insertions disrupted the soluble DegS/DegU two-component system that regulates diverse processes, including competence, biofilm formation, degradative enzymes, motility, and PGA production (80–88).

One way in which PGA production might be regulated is by altering expression of *pgdS* (also known as *ywtD*), encoding PgdS, an enzyme that antagonizes accumulation of PGA by depolymerization (27). To determine if PGA degradation was differentially regulated, the promoter of *pgdS* (P_{pgdS}) was fused to *lacZ* and integrated at the ectopic *amyE* locus in the various mutant backgrounds (*amyE*::P_{pgdS}-*lacZ*). Cells mutated for *motA* had a slightly reduced expression of *pgdS* compared to the wild type (Fig. 4A). As a control, expression of *pgdS* was reduced to background levels in cells mutated for σ^D (*sigD*), the sigma factor that directs *pgdS* expression (Fig. 4A). We infer that the slight decrease in the expression of the PgdS enzyme that degrades PGA does not account for the seemingly dramatic increase in PGA production in the *motA* mutant. Furthermore, simultaneous mutation of *motA* and any of the mutations that abolished mucoidy did not substantially increase *pgdS* expression (Fig. 4A). We infer that an increase in PgdS expression does not account for the loss of mucoidy in the *motA* double mutants.

TABLE 3 Transposon insertions outside of the *pgs* operon that reduced mucoidy in a *motA* mutant

Gene and mutant class	Function of gene product	Transposon[a]	Insertion site[b]
Class 1: flagellar filament			
fliD	FliD, flagellar filament cap	TnΩDS*7755*	TAGCTGTCA
		TnΩDS*8122*	TACTAGCTC
		TnΩDS*8574*	TATAGTCTC
		TnΩDS*8939*	TACGATATC
fliT	FliT, putative FliD chaperone	TnΩDS*7753*	TATAAGGGT
		TnΩDS*8572*	TAATATGTG
flgL	FlgL, hook-associated protein	TnΩDS*8573*	TAACTGCTT
		TnΩDS*9627*	TAAGTTCCG
Class 2: Mfd			
mfd	Mfd, transcription-repair coupling factor	TnΩDS*8656*	TAATCTCCA
		TnΩDS*8691*	TAACTCTGT
		TnΩDS*8935*	TAAGGGTCT
		TnΩDS*8938*	TAGCATAAC
		TnΩDS*8940*	TATCAATTT
		TnΩDS*8985*	TAATCGCTG
Class 3: transcriptional regulators			
codY	CodY, transcriptional pleiotropic repressor	TnΩDS*9018*	TAGATTTTC
comQ	ComQ, ComX modification protein	TnΩDS*9020*	TATCCCCCT
		TnΩDS*9022*	TATCTGCTC*
comX	ComX, competence pheromone precursor	TnΩDS*8971*	TATAAGGCA
comP	ComP, ComX sensor kinase (membrane bound)	TnΩDS*8654*	TATATGCTA
		TnΩDS*8936*	TATATATGC
		TnΩDS*8972*	TAAAAAATC
		TnΩDS*9382*	TATTAAAAA
		TnΩDS*9383*	TATAAAGGA
degS	DegS, sensor kinase (soluble)	TnΩDS*8689*	TACTTGAAT
		TnΩDS*9019*	TACAGTCAA
degU	DegU, response regulator transcription factor	TnΩDS*8701*	TATATAGAA*
		TnΩDS*9021*	TAACCTCTC

[a] The number following TnΩ indicates the strain number within which the transposon is inserted.
[b] The transposon sequence tag, including the TA within which the transposon has inserted and 7 bp downstream for site identification. The asterisk indicates that the insertion is upstream of the gene.

Another way in which PGA production may be regulated is by altering expression of the *pgs* operon encoding the enzymes that synthesize PGA. To measure expression of the *pgs* operon, a transcriptional fusion to the *lacZ* gene encoding β-galactosidase was Campbell integrated downstream of the *pgs* operon at the native site in the chromosome (*pgsEΩlacZ*). Transcription of the *pgs* operon was very low in the wild type but increased almost 4-fold when *motA* was mutated (Fig. 4B). Cells mutated for *motA* and *pgsB*, *mfd*, *codY*, *comQ*, *comX*, *comP*, *degS*, or *degU* reduced expression of the *pgs* operon to levels equivalent to or lower than that for the wild-type cells (Fig. 4B). We infer that the almost 4-fold increase in *pgs* operon expression is at least partly responsible for mucoidy in the *motA* mutant and that reduction of *pgs* operon expression explains the loss of mucoidy in the aforementioned mutants. In contrast, cells mutated for *motA* and *fliD*, *fliT*, or *flgL* did not reduce expression of the *pgs* operon (Fig. 4B). We infer that disruptions in genes related to FliD filament cap assembly reduce PGA overproduction by an alternative mechanism.

Expression of the *pgs* operon is activated by phosphorylated DegU (DegU-P) that binds upstream of the P_{pgsB} promoter (87). DegQ is a ComPA-regulated protein that enhances the phosphorylation of DegU by DegS (85, 89, 90, 91). To test epistatic relationships to DegU, the gene encoding DegQ, *degQ*, was cloned downstream of the IPTG-inducible $P_{hyspank}$ promoter integrated at the ectopic *amyE* site in the mutant backgrounds that reduced production of PGA (*amyE*::$P_{hyspank}$-*degQ*). Induction of DegQ by IPTG restored mucoidy to many of the *motA* double mutants (Fig. 3B). Only three of the mutants did not regain mucoidy in the presence of IPTG: *pgsB*, which is required for PGA synthesis, and *degS* and *degU*, which encode the DegS and DegU two-component system through which DegQ is thought to act (85, 90, 91). We conclude that DegS and DegU are likely the most downstream regulators in *pgs* operon expression, as increased activity of the two-component system can override the other mutants defective in PGA production.

DISCUSSION

Flagellar rotation is powered by the consumption of an ion motive force through membrane-bound stator complexes (2). Stator association with the flagellum is dynamic, and paralogous stators may be substituted, for example, during the transition from swimming to swarming motility of *Pseudomonas aeruginosa* (3, 8, 38, 40, 92). *Bacillus subtilis* swims in liquid media and swarms atop solid surfaces, and it encodes two sets of proteins, MotA/MotB and MotP/MotS, that resemble the flagellar stator (37, 39). Here, we show that the MotA/MotB complex is required for motility but the MotP/MotS complex is not. MotA and MotB are coexpressed with flagellar genes, and we show that mutating conserved resi-

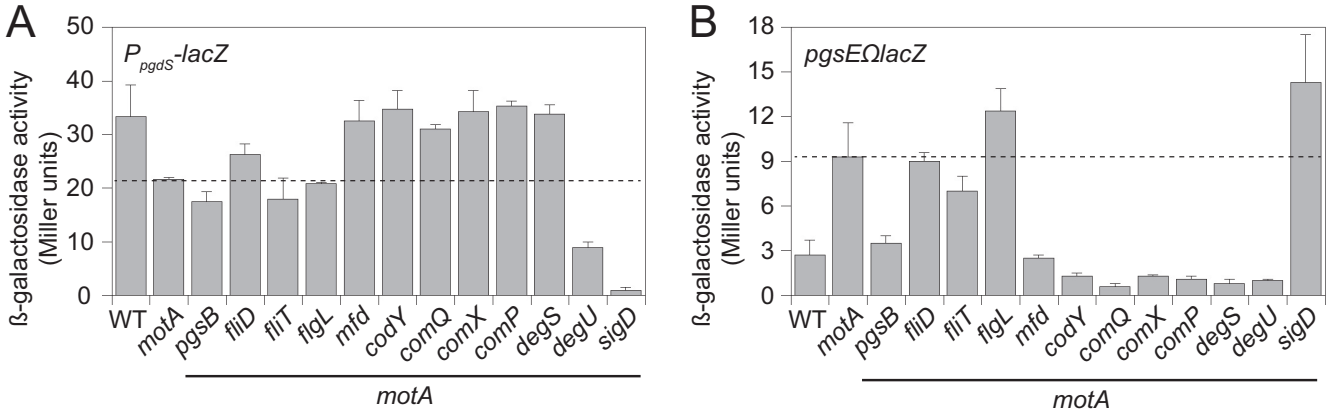

FIG 4 Expression of the PGA biosynthetic operon is increased in a Δ*motA* mutant and reduced in some mutants that abolish mucoidy. (A) β-Galactosidase assays of the P_{pgdS}-*lacZ* transcriptional reporter for the expression of the PgdS enzyme that degrades PGA. The following strains were used to generate this panel: wild type (DS9309), *motA* (DS9349), *motA fliD* (DS9699), *motA fliT* (DS9700), *motA flgL* (DS9736), *motA pgsB* (DS9739), *motA mfd* (DS9704), *motA codY*::Tn (DS9453), *motA comQ* (DS9701), *motA comX* (DS9811), *motA comP* (DS9812), *motA degS* (DK1575), *motA degU* (DS9703), and *motA sigD* (DK1574). (B) β-Galactosidase assays of the *pgsEΩlacZ* transcriptional reporter to monitor expression of the *pgs* operon encoding enzymes that synthesize PGA. The following strains were used to generate this panel: WT (DS9079), *motA* (DS8968), *motA fliD* (DS9691), *motA fliT* (DS9692), *motA flgL* (DS9735), *motA pgsB* (DS9738), *motA mfd* (DS9696), *motA codY*::Tn (DS9134), *motA comQ* (DS9693), *motA comX* (DS9809), *motA comP* (DS9810), *motA degS* (DK1573), *motA degU* (DS9695), and *motA sigD* (DK1572). Error bars are the standard deviations from three replicates. For both panels, the dashed line indicates the level of expression found in the *motA* mutant.

dues of the MotA/MotB stator proteins in *B. subtilis* confers loss-of-function and reduced-function phenotypes similar to those of their counterparts in *E. coli* (17, 37). MotP and MotS, in contrast, are not coregulated with flagellar genes (97, 113), and no suppressors of *motA-motB* deletion mutants were isolated, suggesting that MotA and MotB could not be substituted. We conclude that *B. subtilis* encodes only one set flagellar stator proteins and that the mechanism of stator force generation is highly conserved from the *Proteobacteria* to the *Firmicutes*.

Flagellar stator mutants in *B. subtilis* not only abolished motility but also increased PGA synthesis, resulting in a mucoid colony phenotype. PGA is a secreted homopolymer of glutamate in which the amino group of the amino acid backbone forms a peptide bond with the side chain carboxyl group of another residue (20). In *B. anthracis*, PGA is a cell-associated capsule required for virulence, whereas in *B. subtilis*, PGA is a slime layer of unknown function that is required for some forms of biofilm formation (44, 90, 95). Whatever the mechanistic role of PGA, we infer it is related to the hygroscopic and viscous properties of the material. Why production of PGA would be inhibited by the flagellar stator is unknown.

Inhibition of PGA synthesis by the flagellar stator appears to be due, at least in part, to transcriptional gene regulation, as cells mutated for *motA* experienced a roughly 4-fold increase in *pgs* operon expression (Fig. 4B and Fig. 5). Consistent with previous reports, mutation of the DegS/DegU two-component systems abolished mucoidy in a *motA* background and reduced *pgs* expression to background levels (85, 87, 91). Transcription of *pgs* was similarly reduced when a *motA* background was also mutated for the Com quorum-sensing system, CodY, a nutrition-responsive transcription factor, or Mfd, a transcription-coupled DNA repair protein (62, 71, 89). DegU appears to be the most downstream regulator of *pgs* expression, as mutants defective in ComQXP, CodY, and Mfd were bypassed by artificial expression of DegQ. How the proteins that act upstream of DegU integrate to control mucoidy is unknown, and it is not clear whether these proteins also regulate the other DegU targets. Finally, the input for the soluble kinase DegS that phosphorylates DegU is unknown, but at least two reports have suggested that DegS activation has something to do with flagellar assembly and/or function (48, 88).

Disruptions of three proteins involved in flagellar filament assembly, FlgL, FliT, and FliD, were also found to abolish mucoidy in a flagellar stator mutant background (Fig. 3B and 5). FliD is

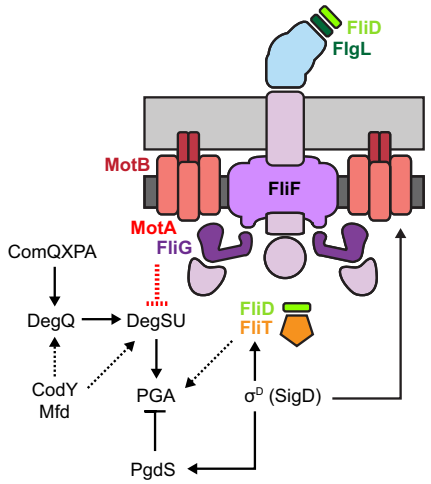

FIG 5 Flagellar motor inhibits PGA synthesis. Cartoon model of the *B. subtilis* flagellum with the location of relevant proteins indicated as matching colored text and symbols. Peptidoglycan is indicated in light gray, membrane is indicated in dark gray, the flagellar basal body is colored purple, and the flagellar hook is colored light blue. Genetic formalisms indicate the regulatory relationships of proteins mentioned in the text. Arrows indicate activation/promotion; T bars indicate repression/inhibition. Solid lines indicate empirical support for regulation, and dashed lines support by inference where the mechanism of regulation is unknown.

secreted by the flagellar basal body with the aid of the putative chaperone FliT and loaded onto the hook-filament junction protein FlgL (51, 53, 54, 56, 57). Once loaded, FliD is the flagellar cap that chaperones flagellin for filament polymerization (50, 52). Recently, the structural protein flagellin has been shown to play a direct role in its autoregulation; thus, FliD may also be regulatory (96). FliD could be the input to DegS, but this seems unlikely, as mutation of *fliD*, *flgL*, or *fliT* in the *motA* background did not phenocopy the *degS* mutant for *pgs* operon expression. In *S. enterica*, the FliD chaperone FliT has a second function in which it directly antagonizes the master activator FlhDC to inhibit flagellar basal body gene expression (97). *B. subtilis*, however, does not encode FlhDC, and the function of FliT is unknown. Ultimately, the roles of FliD, FlgL, and FliT in the activation of PGA are unclear, save that they appear to act by a different mechanism than the other transcriptional regulators, as their presence or absence seems to have no effect on the expression of the PGA synthesis or turnover genes. We note that similar insertions (*flgK*, *fliD*, and *fliT*) were identified previously in a screen for mutations that increased σ^D-dependent gene expression (98).

σ^D-dependent gene expression controls PGA production at multiple levels, and cells mutated for σ^D are mucoid (Fig. 2E and 5). σ^D directs the expression of both the newly identified inhibitors (MotA and MotB) and enhancers (FliD, FlgL, and FliT) of PGA synthesis such that mutation of the gene encoding σ^D (*sigD*) seems to be neutralizing with respect to PGA. σ^D, however, also activates the expression of the PGA-hydrolyzing enzyme PgdS, and we suspect that the *sigD* mutant is mucoid, because the reduction of PgdS permits accumulation of however little PGA is made (Fig. 4) (93). A lack of PgdS expression may also account for why artificial expression of *motA* and *motB* reduces but does not completely inhibit PGA accumulation in the *sigD* background (Fig. 2E). In contrast, artificial expression of *motA* and *motB* in cells mutated for either the FliF or FliG basal body proteins does not appear to cause any reduction in mucoidy. We infer that assembling MotA and MotB onto the basal body, made in part of FliF and FliG, is required for proton conductance and subsequent torque; thus, our data support the recent proposition that flagellar rotation inhibits PGA synthesis (48).

The inhibition of flagellar rotation has been shown to have regulatory consequences in various bacteria. For example, impedance on the sodium-driven polar flagellum induces the expression of proton-driven peritrichous (lateral) flagella during swarming in *Vibrio parahaemolyticus* (99–102). Similarly, the single flagellar system of swarming *Proteus mirabilis* is thought to be activated by surface contact sensing through a protein that may interact with the flagellar motor (103–106). Besides control over flagella themselves, flagellum-dependent regulation in response to surface contact has been shown to control virulence gene expression (107, 108). Here, we find that inhibition of the *B. subtilis* flagellar stator leads to the production of an extracellular polymer, perhaps akin to the way the inhibition of flagellar rotation of *Caulobacter crescentus* leads to production of the adhesive holdfast polysaccharide (109). How flagellar rotation is being sensed is not known for any system, but recent reports have suggested that the number of stators associated with the flagellum increases with increasing rotational resistance experienced upon surface contact (110, 111). We however note that models invoking an increase in stator association and, therefore, proton conductance seem unlikely to explain how loss-of-conductance mutants cause mucoidy in *B. subtilis*.

Why and how the *B. subtilis* flagellar stator regulates PGA synthesis is unknown, but PGA overproduction is practical. PGA is a side product in the fermentation of soybeans and other food products and is a useful polymer for biomedical and industrial applications as a food additive, metal chelator, gelling agent, adjuvant, or adhesive (112, 113). Efforts have been made to improve PGA yields from *B. subtilis* strains, and mutation of the flagellar stator is one potential improvement. In fact, many strains of *B. subtilis* subspecies *natto* used for soybean fermentation due to their high PGA yields are also nonmotile. Our work suggests that the relationship of a lack of motility to enhanced PGA synthesis is causal rather than coincidental.

ACKNOWLEDGMENTS

We are grateful to Rebecca Calvo and Melissa Konkol for strain construction and experimental support.

This work was supported by NIH grant GM093030 to D.B.K.

REFERENCES

1. **Chevance FFV, Hughes KT.** 2008. Coordinating assembly of a bacterial macromolecular machine. Nat. Rev. Microbiol. **6:**455–465. http://dx.doi.org/10.1038/nrmicro1887.
2. **Berg HC.** 2003. The rotary motor of bacterial flagella. Annu. Rev. Biochem. **72:**19–54. http://dx.doi.org/10.1146/annurev.biochem.72.121801.161737.
3. **Blair DF, Berg HC.** 1988. Restoration of torque in defective flagellar motors. Science **242:**1678–1681. http://dx.doi.org/10.1126/science.2849208.
4. **Khan S, Dapice M, Reese TS.** 1988. Effects of *mot* gene expression on the structure of the flagellar motor. J. Mol. Biol. **202:**575–584. http://dx.doi.org/10.1016/0022-2836(88)90287-2.
5. **Berg HC, Turner L.** 1993. Torque generated by the flagellar motor of *Escherichia coli*. Biophys. J. **65:**2201–2216. http://dx.doi.org/10.1016/S0006-3495(93)81278-5.
6. **Gabel CV, Berg HC.** 2003. The speed of the flagellar rotary motor of *Escherichia coli* varies linearly with proton motive force. Proc. Natl. Acad. Sci. U. S. A. **100:**8748–8751. http://dx.doi.org/10.1073/pnas.1533395100.
7. **Reid SW, Leake MC, Chandler JH, Lo CJ, Armitage JP, Berry RM.** 2006. The maximum number of torque-generating units in the flagellar motor of *Escherichia coli* is at least 11. Proc. Natl. Acad. Sci. U. S. A. **103:**8066–8071. http://dx.doi.org/10.1073/pnas.0509932103.
8. **Block SM, Berg HC.** 1984. Successive incorporation of force generating units in the bacterial rotary motor. Nature **309:**470–472. http://dx.doi.org/10.1038/309470a0.
9. **Kojima S, Blair DF.** 2004. Solubilization and purification of the MotA/MotB complex of *Escherichia coli*. Biochemistry **43:**26–34. http://dx.doi.org/10.1021/bi035405l.
10. **Chun SY, Parkinson JS.** 1988. Bacterial motility: membrane topology of the *Escherichia coli* MotB protein. Science **239:**276–278. http://dx.doi.org/10.1126/science.2447650.
11. **Zhou J, Sharp Tang LL, Lloyd HL SA, Billings S, Braun TY, Blair DF.** 1998. Function of protonatable residues in the flagellar motor of *Escherichia coli*: a critical role for Asp 32 of MotB. J. Bacteriol. **180:**2729–2735.
12. **Kojima S, Imada K, Sakuma M, Sudo Y, Kojima C, Minamino T, Homma M, Namba K.** 2009. Stator assembly and activation mechanism of the flagella motor by the periplasmic region of MotB. Mol. Microbiol. **73:**710–718. http://dx.doi.org/10.1111/j.1365-2958.2009.06802.x.
13. **Zhou J, Fazzio RT, Blair DF.** 1995. Membrane topology of the MotA protein of *Escherichia coli*. J. Mol. Biol. **251:**237–242. http://dx.doi.org/10.1006/jmbi.1995.0431.
14. **Kojima S, Blair DF.** 2001. Conformational change in the stator of the bacterial flagellar motor. Biochemistry **40:**13041–13050. http://dx.doi.org/10.1021/bi011263o.
15. **Garza AG, Harris-Haller LW, Stoebner RA, Manson MD.** 1995. Motility protein interactions in the bacterial flagellar motor. Proc. Natl. Acad. Sci. U. S. A. **92:**1970–1974. http://dx.doi.org/10.1073/pnas.92.6.1970.
16. **Lee LK, Ginsburg MA, Crovace C, Donohoe M, Stock D.** 2010. Structure of the torque ring of the flagellar motor and the molecular basis for rotational switching. Nature **466:**996–1000. http://dx.doi.org/10.1038/nature09300.

17. **Zhou J, Blair DF.** 1997. Residues of the cytoplasmic domain of MotA essential for torque generation in the bacterial flagellar motor. J. Mol. Biol. **273:**428–439. http://dx.doi.org/10.1006/jmbi.1997.1316.
18. **Zhou J, Lloyd SA, Blair DF.** 1998. Electrostatic interactions between rotor and stator in the bacterial flagellar motor. Proc. Natl. Acad. Sci. U. S. A. **95:**6436–6441. http://dx.doi.org/10.1073/pnas.95.11.6436.
19. **Candela T, Fouet A.** 2006. Poly-gamma-glutamate in bacteria. Mol. Microbiol. **60:**1091–1098. http://dx.doi.org/10.1111/j.1365-2958.2006.05179.x.
20. **Bovarnick M.** 1942. The formation of extracellular d(-)-glutamic acid polypeptide by *Bacillus subtilis*. J. Biol. Chem. **145:**415–424.
21. **Hanby WE, Rydon HN.** 1946. The capsular substance of *Bacillus anthracis*. Biochem. J. **40:**297–309.
22. **Candela T, Fouet A.** 2005. *Bacillus anthracis* CapD, belonging to the γ-glutamyltranspeptidase family, is required for the covalent anchoring of capsule to peptidoglycan. Mol. Microbiol. **57:**717–726. http://dx.doi.org/10.1111/j.1365-2958.2005.04718.x.
23. **Makino SI, Uchida I, Terakado N, Sasakawa C, Yoshikawa M.** 1989. Molecular characterization and protein analysis of the *cap* region, which is essential for encapsulation in *Bacillus anthracis*. J. Bacteriol. **171:**722–730.
24. **Ashiuchi M, Soda K, Misono H.** 1999. A poly-γ-glutamate synthetic system of *Bacillus subtilis* IFO 3336: gene cloning and biochemical analysis of poly-γ-glutamate produced by *Escherichia coli* clone cells. Biochem. Biophys. Res. Commun. **263:**6–12. http://dx.doi.org/10.1006/bbrc.1999.1298.
25. **Urushibata Y, Tokuyama S, Tahara Y.** 2002. Characterization of the *Bacillus subtilis ywsC* gene, involved in γ-polyglutamic acid production. J. Bacteriol. **184:**337–343. http://dx.doi.org/10.1128/JB.184.2.337-343.2002.
26. **Kimura K, Tran LSP, Do TH, Itoh Y.** 2009. Expression of *pgsB* encoding the poly gamma-DL-glutamate of *Bacillus subtilis natto*. Biosci. Biotechnol. Biochem. **73:**1149–1155. http://dx.doi.org/10.1271/bbb.80913.
27. **Suzuki T, Tahara Y.** 2003. Characterization of the *Bacillus subtilis ywtD* gene, whose product is involved in γ-polyglutamic acid degradation. J. Bacteriol. **185:**2379–2382. http://dx.doi.org/10.1128/JB.185.7.2379-2382.2003.
28. **Ashiuchi M, Nakamura H, Yamamoto M, Misono H.** 2006. Novel poly-γ-glutamate-processing enzyme catalyzing γ-glutamyl DD-amidohydrolysis. J. Biosci. Bioeng. **1:**60–65. http://dx.doi.org/10.1263/jbb.102.60.
29. **Le Breton Y, Mohapatra NP, Haldenwang WG.** 2006. *In vivo* random mutagenesis of *Bacillus subtilis* by use of TnYLB-1, a mariner-based transposon. Appl. Environ. Microbiol. **72:**327–333. http://dx.doi.org/10.1128/AEM.72.1.327-333.2006.
30. **Tran LSP, Nagai T, Itoh Y.** 2000. Divergent structure of the ComQXPA quorum-sensing components: molecular basis of strain-specific communication mechanism in *Bacillus subtilis*. Mol. Microbiol. **37:**1159–1171. http://dx.doi.org/10.1046/j.1365-2958.2000.02069.x.
31. **Yasbin RE, Young FE.** 1974. Transduction in *Bacillus subtilis* by Bacteriophage SPP1. J. Virol. **14:**1343–1348.
32. **Patrick JE, Kearns DB.** 2008. MinJ (YvjD) is a topological determinant of cell division in *Bacillus subtilis*. Mol. Microbiol. **70:**1166–1179. http://dx.doi.org/10.1111/j.1365-2958.2008.06469.x.
33. **Ben-Yehuda S, Rudner DZ, Losick R.** 2003. RacA, a bacterial protein that anchors chromosomes to cell poles. Science **299:**532–536. http://dx.doi.org/10.1126/science.1079914.
34. **Antoniewski C, Savelli B, Stragier P.** 1990. The *spoIIJ* gene, which regulates early developmental steps in *Bacillus subtilis*, belongs to a class of environmentally responsive genes. J. Bacteriol. **172:**86–93.
35. **Guérout-Fleury AM, Shazand K, Frandsen N, Stragier P.** 1995. Antibiotic resistance cassettes for *Bacillus subtilis*. Gene **167:**335–336. http://dx.doi.org/10.1016/0378-1119(95)00652-4.
36. **Wach A.** 1996. PCR-synthesis of marker cassettes with long flanking homology regions for gene disruptions in *S. cerevisiae*. Yeast **12:**259–265.
37. **Mirel DB, Lustre VM, Chamberlin MJ.** 1992. An operon of *Bacillus subtilis* motility genes transcribed by the σ^D form of RNA polymerase. J. Bacteriol. **174:**4197–4204.
38. **Doyle TB, Hawkins AC, McCarter LL.** 2004. The complex flagellar torque generator of *Pseudomonas aeruginosa*. J. Bacteriol. **186:**6341–6350. http://dx.doi.org/10.1128/JB.186.19.6341-6350.2004.
39. **Ito M, Hicks DB, Henkin TM, Guffanti AA, Powers BD, Zvi L, Uematsu K, Krulwich TA.** 2004. MotPS is the stator-force generator for motility of alkaliphilic *Bacillus*, and its homologue is a second functional Mot in *Bacillus subtilis*. Mol. Microbiol. **53:**1035–1049. http://dx.doi.org/10.1111/j.1365-2958.2004.04173.x.
40. **Toutain CM, Zegans ME, O'Toole GA.** 2005. Evidence for two flagellar stators and their role in the motility of *Pseudomonas aeruginosa*. J. Bacteriol. **187:**771–777. http://dx.doi.org/10.1128/JB.187.2.771-777.2005.
41. **Ito M, Terahara N, Fujinami S, Krulwich TA.** 2005. Properties of motility in *Bacillus subtilis* powered by the H^+-coupled MotAB flagellar stator, Na^+-coupled MotPS or hybrid stators MotAS or MotPB. J. Mol. Biol. **352:**396–408. http://dx.doi.org/10.1016/j.jmb.2005.07.030.
42. **Cosmina P, Rodriguez F, de Ferra F, Grandi G, Perego M, Venema G, van Sinderen D.** 1993. Sequence and analysis of the genetic locus responsible for surfactin synthesis in *Bacillus subtilis*. Mol. Microbiol. **8:**821–831. http://dx.doi.org/10.1111/j.1365-2958.1993.tb01629.x.
43. **Branda SS, Gonzalez-Pastor JE, Ben-Yehuda S, Losick R, Kolter R.** 2001. Fruiting body formation by *Bacillus subtilis*. Proc. Natl. Acad. Sci. U. S. A. **98:**11621–11626. http://dx.doi.org/10.1073/pnas.191384198.
44. **Branda SS, Chu F, Kearns DB, Losick R, Kolter R.** 2006. A major protein component of the *Bacillus subtilis* biofilm matrix. Mol. Microbiol. **59:**1229–1238. http://dx.doi.org/10.1111/j.1365-2958.2005.05020.x.
45. **Kearns DB, Chu F, Branda SS, Kolter R, Losick R.** 2005. A master regulator for biofilm formation by *Bacillus subtilis*. Mol. Microbiol. **55:**739–749. http://dx.doi.org/10.1111/j.1365-2958.2004.04440.x.
46. **Kobayashi K, Iwano M.** 2012. BslA (YuaB) forms a hydrophobic layer on the surface of *Bacillus subtilis* biofilms. Mol. Microbiol. **85:**51–66. http://dx.doi.org/10.1111/j.1365-2958.2012.08094.x.
47. **Hobley L, Ostrowski A, Rao FV, Bromley KM, Porter M, Prescott AR, MacPhee CE, van Aalten DMF, Stanley-Wall NR.** 2013. BslA is a self-assembling bacterial hydrophobin that coats the *Bacillus subtilis* biofilm. Proc. Natl. Acad. Sci. U. S. A. **110:**13600–13605. http://dx.doi.org/10.1073/pnas.1306390110.
48. **Cairns LS, Marlow VL, Bissett E, Ostrowski A, Stanley-Wall NR.** 2013. A mechanical signal transmitted by the flagellum controls signaling in *Bacillus subtilis*. Mol. Microbiol. **90:**6–21. http://dx.doi.org/10.1111/mmi.12342.
49. **Barilla D, Caramori T, Galizzi A.** 1994. Coupling of flagellin gene transcription to flagellar assembly in *Bacillus subtilis*. J. Bacteriol. **176:**4558–4564.
50. **Yokoseki T, Kutsukake K, Ohnishi K, Iino T.** 1995. Functional analysis of the flagellar genes in the *fliD* operon of *Salmonella typhimurium*. Microbiology **141:**1715–1722. http://dx.doi.org/10.1099/13500872-141-7-1715.
51. **Ikeda T, Oosawa K, Hotani H.** 1996. Self-assembly of the filament capping protein, FliD, of bacterial flagella into an annular structure. J. Mol. Biol. **259:**679–686. http://dx.doi.org/10.1006/jmbi.1996.0349.
52. **Mukherjee S, Babitzke P, Kearns DB.** 2013. FliW and FliS function independently to control cytoplasmic flagellin levels in *Bacillus subtilis*. J. Bacteriol. **195:**297–306. http://dx.doi.org/10.1128/JB.01654-12.
53. **Fraser GM, Bennett JCQ, Hughes C.** 1999. Substrate-specific binding of hook-associated proteins bu FlgN and FliT, putative chaperones for flagellum assembly. Mol. Microbiol. **32:**569–580. http://dx.doi.org/10.1046/j.1365-2958.1999.01372.x.
54. **Bennett JCQ, Thomas J, Fraser GM, Hughes C.** 2001. Substrate complexes and domain organization of the *Salmonella* flagellar export chaperones FlgN and FliT. Mol. Microbiol. **39:**781–791. http://dx.doi.org/10.1046/j.1365-2958.2001.02268.x.
55. **Homma M, Kutsukake K, Iino T, Yamaguchi S.** 1984. Hook-associated proteins essential for flagellar filament formation in *Salmonella typhimurium*. J. Bacteriol. **157:**100–108.
56. **Homma M, Fukita H, Yamaguchi S, Iino T.** 1984. Excretion of unassembled flagellin by *Salmonella typhimurium* mutants deficient in hook-associated proteins. J. Bacteriol. **159:**1056–1059.
57. **Ikeda T, Yamaguchi S, Hotani H.** 1993. Flagellar growth in a filamentless *Salmonella fliD* mutant supplemented with purified hook-associated protein 2. J. Biochem. **114:**39–44.
58. **Mellon I, Spivak G, Hanawalt PC.** 1987. Selective removal of transcription-blocking DNA damage from the transcribed strand of the mammalian DHFR gene. Cell **51:**241–249. http://dx.doi.org/10.1016/0092-8674(87)90151-6.
59. **Mellon I, Hanawalt PC.** 1989. Induction of the *Escherichia coli* lactose operon selectively increases repair of its transcribed DNA strand. Nature **342:**95–98. http://dx.doi.org/10.1038/342095a0.
60. **Selby CP, Witkin EM, Sancar A.** 1991. *Escherichia coli mfd* mutant deficient in "mutation frequency decline" lacks strand-specific repair: *in*

vitro complementation with purified coupling factor. Proc. Natl. Acad. Sci. U. S. A. **88:**11574–11578. http://dx.doi.org/10.1073/pnas.88.24.11574.
61. **Oller AR, Fijalkowska IJ, Dunn RL, Schaaper RM.** 1992. Transcription-repair coupling determines the strandedness of ultraviolet mutagenesis in *Escherichia coli*. Proc. Natl. Acad. Sci. U. S. A. **89:**11036–11040. http://dx.doi.org/10.1073/pnas.89.22.11036.
62. **Savery NJ.** 2007. The molecular mechanism of transcription-coupled DNA repair. Trends Microbiol. **15:**326–333. http://dx.doi.org/10.1016/j.tim.2007.05.005.
63. **Selby CP, Sancar A.** 1993. Molecular mechanism of transcription-repair coupling. Science **260:**53–57. http://dx.doi.org/10.1126/science.8465200.
64. **Selby CP, Sancar A.** 1995. Structure and function of transcription-repair coupling factor. J. Biol. Chem. **270:**4882–4889. http://dx.doi.org/10.1074/jbc.270.9.4882.
65. **Ayora S, Rojo F, Ogasawara N, Nakai S, Alonso JC.** 1996. The Mfd protein of *Bacillus subtilis* 168 is involved in both transcription-coupled DNA repair and DNA recombination. J. Mol. Biol. **256:**301–318. http://dx.doi.org/10.1006/jmbi.1996.0087.
66. **Park JS, Marr MT, Roberts JW.** 2002. *E. coli* transcription repair coupling factor (Mfd protein) rescues arrested complexes by promoting forward translocation. Cell **109:**757–767. http://dx.doi.org/10.1016/S0092-8674(02)00769-9.
67. **Trautinger BW, Jaktaji RP, Rusakova E, Lloyd RG.** 2005. RNA polymerase modulator and DNA repair activities resolve conflicts between DNA replication and transcription. Cell **19:**247–258. http://dx.doi.org/10.1016/j.molcel.2005.06.004.
68. **Pomerantz RT, O'Donnell M.** 2010. Direct restart of a replication fork stalled by a head-on RNA polymerase. Science **327:**590–592. http://dx.doi.org/10.1126/science.1179595.
69. **Zalieckas JM, Wray LV, Jr, Ferson AE, Fisher LH.** 1998. Transcription-repair coupling factor is involved in carbon catabolite repression of the *Bacillus subtilis hut* and *gnt* operons. Mol. Microbiol. **27:**1031–1038. http://dx.doi.org/10.1046/j.1365-2958.1998.00751.x.
70. **Belitsky BR, Sonenshein AL.** 2011. Roadblock repression of transcription by *Bacillus subtilis* CodY. J. Mol. Biol. **411:**729–743. http://dx.doi.org/10.1016/j.jmb.2011.06.012.
71. **Ratnayake-Lecamwasam M, Serror P, Wong KW, Sonenshein AL.** 2001. *Bacillus subtilis* CodY represses early-stationary-phase genes by sensing GTP levels. Genes Dev. **15:**1093–1103. http://dx.doi.org/10.1101/gad.874201.
72. **Molle V, Nakaura Y, Shivers RP, Yamaguchi H, Losick R, Fujita Y, Sonenshein A.** 2003. Additional targets of the *Bacillus subtilis* global regulator CodY identified by chromatin immunoprecipitation and genome-wide transcript analysis. J. Bacteriol. **185:**1911–1922. http://dx.doi.org/10.1128/JB.185.6.1911-1922.2003.
73. **Shivers RP, Sonenshein AL.** 2004. Activation of the *Bacillus subtilis* global regulator CodY by direct interaction with branched-chain amino acids. Mol. Microbiol. **53:**599–611. http://dx.doi.org/10.1111/j.1365-2958.2004.04135.x.
74. **Solomon JM, Magnuson R, Srivastava A, Grossman AD.** 1995. Convergent sensing pathways mediate response to two extracellular competence factors in *Bacillus subtilis*. Genes Dev. **9:**547–558. http://dx.doi.org/10.1101/gad.9.5.547.
75. **Bacon Schneider K, Palmer TM, Grossman AD.** 2002. Characterization of *comQ* and *comX*, two genes required for production of ComX pheromone in *Bacillus subtilis*. J. Bacteriol. **184:**410–419. http://dx.doi.org/10.1128/JB.184.2.410-419.2002.
76. **Magnuson R, Solomon J, Grossman AD.** 1994. Biochemical and genetic characterization of a competence pheromone from *B. subtilis*. Cell **77:**207–216. http://dx.doi.org/10.1016/0092-8674(94)90313-1.
77. **Tsuji F, Ishihara A, Kurata K, Nakagawa A, Okada M, Kitamura S, Kanamaru K, Masuda Y, Murakami K, Irie K, Sakagami Y.** 2012. Geranyl modification on the tryptophan residue of $ComX_{RO-E-2}$ pheromone by a cell free system. FEBS Lett. **586:**174–179. http://dx.doi.org/10.1016/j.febslet.2011.12.012.
78. **Weinrauch Y, Penchev R, Dubnau E, Smith I, Dubnau D.** 1990. A *Bacillus subtilis* regulatory gene product for genetic competence and sporulation resembles sensor protein members of the bacterial two-component signal-transduction systems. Genes Dev. **4:**860–872. http://dx.doi.org/10.1101/gad.4.5.860.
79. **Piazza F, Tortosa P, Dubnau D.** 1999. Mutational analysis and membrane topology of ComP, a quorum-sensing histidine kinase of *Bacillus subtilis* controlling competence development. J. Bacteriol. **181:**4540–4548.
80. **Msadek T, Kunst F, Henner D, Klier A, Rapoport G, Dedonder R.** 1990. Signal transduction pathway controlling synthesis of a class of degradative enzymes in *Bacillus subtilis*: expression of the regulatory genes and analysis of mutations in *degS* and *degU*. J. Bacteriol. **172:**824–834.
81. **Dahl MK, Msadek T, Kunst F, Rapoport G.** 1991. Mutational analysis of the *Bacillus subtilis* DegU regulator and its phosphorylation by the DegS protein kinase. J. Bacteriol. **173:**2539–2547.
82. **Dahl MK, Msadek T, Kunst Rapoport FG.** 1992. The phosphorylation state of the DegU response regulator acts as a molecular switch allowing either degradative enzyme synthesis of expression of genetic competence in *Bacillus subtilis*. J. Biol. Chem. **267:**14509–14514.
83. **Hamoen LW, Van Werkhoven AF, Venema G, Dubnau D.** 2000. The pleiotropic response regulator DegU functions as a priming protein in competence development in *Bacillus subtilis*. Proc. Natl. Acad. Sci. U. S. A. **97:**9246–9251. http://dx.doi.org/10.1073/pnas.160010597.
84. **Amati G, Bisicchia P, Galizzi A.** 2004. DegU-P represses expression of the motility *fla/che* operon in *Bacillus subtilis*. J. Bacteriol. **186:**6003–6014. http://dx.doi.org/10.1128/JB.186.18.6003-6014.2004.
85. **Kobayashi K.** 2007. Gradual activation of the response regulator DegU controls serial expression of genes for flagellum formation and biofilm formation in *Bacillus subtilis*. Mol. Microbiol. **66:**395–409. http://dx.doi.org/10.1111/j.1365-2958.2007.05923.x.
86. **Verhamme DT, Kiley TB, Stanley-Wall NR.** 2007. DegU co-ordinates multicellular behaviour exhibited by *Bacillus subtilis*. Mol. Microbiol. **65:**554–568. http://dx.doi.org/10.1111/j.1365-2958.2007.05810.x.
87. **Ohsawa T, Tsukahara K, Ogura M.** 2009. *Bacillus subtilis* response regulator DegU is a direct activator of *pgsB* transcription involved in γ-poly-glutamic acid synthesis. Biosci. Biotechnol. Biochem. **73:**2096–2102. http://dx.doi.org/10.1271/bbb.90341.
88. **Hsueh YH, Cozy LM, Sham LT, Calvo RA, Gutu AD, Winkler ME, Kearns DB.** 2011. DegU-phosphate activates expression of the anti-sigma factor FlgM in *Bacillus subtilis*. Mol. Microbiol. **81:**1092–1108. http://dx.doi.org/10.1111/j.1365-2958.2011.07755.x.
89. **Msadek T, Kunst F, Klier A, Rapoport G.** 1991. DegS-DegU and ComP-ComA modulator-effector pairs control expression of the *Bacillus subtilis* pleiotropic regulatory gene *degQ*. J. Bacteriol. **173:**2366–2377.
90. **Stanley NR, Lazazzera BA.** 2005. Defining the genetic differences between wild and domestic strains of *Bacillus subtilis* that affect poly-γ-DL-glutamic acid production and biofilm formation. Mol. Microbiol. **57:**1143–1158. http://dx.doi.org/10.1111/j.1365-2958.2005.04746.x.
91. **Do TH, Suzuki Y, Abe N, Kaneko J, Itoh Y, Kimura K.** 2011. Mutations suppressing the loss of DegQ function in *Bacillus subtilis natto* poly-γ-glutamate synthesis. Appl. Environ. Microbiol. **77:**8249–8258. http://dx.doi.org/10.1128/AEM.05827-11.
92. **Leake MC, Chandler JH, Wadhams GH, Bai F, Berry RM, Armitage JP.** 2006. Stoichiometry and turnover in single functioning membrane protein complexes. Nature **443:**355–358. http://dx.doi.org/10.1038/nature05135.
93. **Kearns DB, Losick R.** 2005. Cell population heterogeneity during growth of *Bacillus subtilis*. Genes Dev. **19:**3083–3094. http://dx.doi.org/10.1101/gad.1373905.
94. **Nicolas P, Mäder U, Dervyn E, Rochat T, Leduc A, Pigeonneau N, Bidnenko E, Marchadier E, Hoebeke M, Aymerich S, Becher D, Bisicchia P, Botella E, Delumeau O, Doherty G, Denham EL, Fogg MJ, Fromion V, Goelzer A, Hansen A, Härtig E, Harwood CR, Homuth G, Jarmer H, Jules M, Klipp E, Le Chat L, Lecointe F, Lewis P, Liebermeister W, March A, Mars RAT, Nannapaneni P, Noone D, Pohl S, Rinn B, Rügheimer F, Sappa PK, Samson F, Schaffer M, Schwikowski B, Steil L, Stülke J, Wiegert T, Devine KM, Wilkinson AJ, van Dijl M, Hecker M, Völker U, Bessières P, Noirot P.** 2012. Condition-dependent transcriptome reveals high-level regulatory architecture in Bacillus subtilis. Science **335:**1103–1106. http://dx.doi.org/10.1126/science.1206848.
95. **Drysdale M, Heninger S, Hutt J, Chen Y, Lyons CR, Koehler TM.** 2005. Capsule synthesis by *Bacillus anthracis* is required for dissemination in murine inhalation anthrax. EMBO J. **24:**221–227. http://dx.doi.org/10.1038/sj.emboj.7600495.
96. **Mukherjee S, Yakhnin H, Kysela D, Sokoloski J, Babitzke P, Kearns DB.** 2011. CsrA-FliW interaction governs flagellin homeostasis and a checkpoint on flagellar morphogenesis in *Bacillus subtilis*. Mol. Microbiol. **82:**447–461. http://dx.doi.org/10.1111/j.1365-2958.2011.07822.x.

97. **Yamamoto S, Kutsukake K.** 2006. FliT acts as an anti-$FlhD_2C_2$ factor in the transcriptional control of the flagellar regulon in *Salmonella enterica* serovar typhimurium. J. Bacteriol. **188:**6703–6708. http://dx.doi.org/10.1128/JB.00799-06.
98. **Fredrick K, Helmann JD.** 1996. FlgM is a primary regulator of σ^D activity, and its absence restores motility to a *sinR* mutant. J. Bacteriol. **178:**7010–7013.
99. **Belas R, Simon M, Silverman M.** 1986. Regulation of lateral flagella gene transcription in *Vibrio parahaemolyticus*. J. Bacteriol. **167:**210–218.
100. **McCarter L, Hilman M, Silverman M.** 1988. Flagellar dynamometer controls swarmer cell differentiation of *V. parahaemolyticus*. Cell 54:345–351.
101. **Kawagishi I, Imagawa M, Imae Y, McCarter L, Homma M.** 1996. The sodium-driven polar flagellar motor of marine *Vibrio* as the mechanosensor that regulates lateral flagellar expression. Mol. Microbiol. **20:**693–699. http://dx.doi.org/10.1111/j.1365-2958.1996.tb02509.x.
102. **Jaques S, Kim YK, McCarter LL.** 1999. Mutations conferring resistance to phenamil and amiloride, inhibitors of sodium-driven motility of *Vibrio parahaemolyticus*. Proc. Natl. Acad. Sci. U. S. A. **96:**5740–5745. http://dx.doi.org/10.1073/pnas.96.10.5740.
103. **Belas R, Suvanasuthi R.** 2005. The ability of *Proteus mirabilis* to sense surfaces and regulate virulence gene expression involves FliL, a flagellar basal body protein. J. Bacteriol. **187:**6789–6803. http://dx.doi.org/10.1128/JB.187.19.6789-6803.2005.
104. **Jenal U, White J, Shapiro L.** 1994. *Caulobacter* flagellar function, but not assembly, requires FliL, a non-polarly localized membrane protein present in all cell types. J. Mol. Biol. **243:**227–244. http://dx.doi.org/10.1006/jmbi.1994.1650.
105. **Suaste-Olmos F, Domenzain C, Mireles-Rodríguez JC, Poggio S, Osorio A, Dreyfus G, Camarena L.** 2010. The flagellar protein FliL is essential for swimming in *Rhodobacter sphaeroides*. J. Bacteriol. **192:**6230–6239. http://dx.doi.org/10.1128/JB.00655-10.
106. **Lee YY, Patellis J, Belas R.** 2013. Activity of *Proteus mirabilis* FliL is viscosity dependent and requires extragenic DNA. J. Bacteriol. **195:**823–832. http://dx.doi.org/10.1128/JB.02024-12.
107. **Häse C, Mekalanos JJ.** 1999. Effects of changes in membrane sodium flux on virulence gene expression in *Vibrio cholerae*. Proc. Natl. Acad. Sci. U. S. A. **96:**3183–3187. http://dx.doi.org/10.1073/pnas.96.6.3183.
108. **Gode-Potratz CJ, Kustusch RJ, Breheny PJ, Weiss DS, McCarter LL.** 2011. Surface sensing in *Vibrio parahaemolyticus* triggers a programme of gene expression that promotes colonization and virulence. Mol. Microbiol. **79:**240–263. http://dx.doi.org/10.1111/j.1365-2958.2010.07445.x.
109. **Li G, Brown PJ, Tang JX, Xu J, Quardokus EM, Fuqua C, Brun YV.** 2012. Surface contact stimulates the just-in-time deployment of bacterial adhesins. Mol. Microbiol. **83:**41–51. http://dx.doi.org/10.1111/j.1365-2958.2011.07909.x.
110. **Lele PP, Hosu BG, Berg HC.** 2013. Dynamics of mechanosensing in the bacterial flagellar motor. Proc. Natl. Acad. Sci. U. S. A. **110:**11839–11844. http://dx.doi.org/10.1073/pnas.1305885110.
111. **Tipping MJ, Delalez NJ, Lim R, Berry RM, Armitage JP.** 2013. Load-dependent assembly of the bacterial flagellar motor. mBio 4:e00551-13. http://dx.doi.org/10.1128/mBio.00551-13.
112. **Meerak J, Iida H, Watanabe Y, Miyashita M, Sato H, Nakagawa Y, Tahara Y.** 2007. Phylogeny of γ-polyglutamic acid-producing *Bacillus* strains isolated from fermented soybean foods manufactured in Asian countries. J. Gen. Appl. Microbiol. **53:**315–323. http://dx.doi.org/10.2323/jgam.53.315.
113. **Buescher JM, Margaritis A.** 2007. Microbial biosynthesis of polyglutamic acid biopolymer and applications in the biopharmaceutical, biomedical, and food industries. Crit. Rev. Biotechnol. **27:**1–19. http://dx.doi.org/10.1080/07388550601166458.
114. **Pozsgai ER, Blair KM, Kearns DB.** 2012. Modified mariner transposons for random inducible-expression insertions and transcriptional reporter fusion insertions in *Bacillus subtilis*. Appl. Environ. Microbiol. **78:**778–785. http://dx.doi.org/10.1128/AEM.07098-11.
115. **Konkol MA, Blair KM, Kearns DB.** 2013. Plasmid-encoded ComI inhibits competence in the ancestral 3610 strain of *Bacillus subtilis*. J. Bacteriol. **195:**4085–4093. http://dx.doi.org/10.1128/JB.00696-13.
116. **Cozy LM, Phillips AM, Calvo RA, Bate AR, Hsueh Y-H, Bonneau R, Eichenberger P, Kearns DB.** 2012. SlrA/SinR/SlrR inhibits motility gene expression upstream of a hypersensitive and hysteretic switch at the level of σ^D in *Bacillus subtilis*. Mol. Microbiol. **83:**1210–1228. http://dx.doi.org/10.1111/j.1365-2958.2012.08003.x.